

UNIVERSITY OF ILLINOIS

.....**May 15th 92**.....

THIS IS TO CERTIFY THAT THE THESIS PREPARED UNDER MY SUPERVISION BY

.....**Timothy Harold Warren**.....

ENTITLED.....**The Selective Chemical Vapor Deposition of**.....

.....**Silver Films from Metal-Organic Precursors**.....

IS APPROVED BY ME AS FULFILLING THIS PART OF THE REQUIREMENTS FOR THE

DEGREE OF.....**Bachelor of Science in Chemistry**.....

.....*Jacques & Guiseppe -*
.....**Instructor in Charge**.....

APPROVED:.....*[Signature]*.....

HEAD OF DEPARTMENT OF.....**Chemistry**.....

**The Selective Chemical Vapor Deposition of Silver
from Metal-Organic Precursors**

by

Timothy H. Warren

Thesis

for the

Degree of Bachelor of Science

in

Chemistry

College of Liberal Arts and Sciences

University of Illinois

Urbana, Illinois

1992

Table of Contents

Chapter 1: Synthesis and Structure of Silver(I) Acetate and Acetylacetonato Phosphine Complexes: Silver Chemical Vapor Deposition Precursors

Introduction.....	1
Results and Discussion.....	3
Experimental.....	24
References.....	30

Chapter 2: Selective Chemical Vapor Deposition of Silver Films by Transmetalization Reactions

Introduction.....	34
Results and Discussion.....	35
Experimental.....	46
References.....	47

Chapter 1

Synthesis and Structure of Silver(I) Acetate and Acetylacetonate

Phosphine Complexes:

Silver Chemical Vapor Deposition Precursors

Introduction

Few routes to the chemical vapor deposition of silver films have been developed, largely due to the paucity of suitable precursors. Two anonymously published reports describe the deposition of silver from $\text{Ag}(\text{O}_2\text{CCF}_3)$ ¹ and $\text{Ag}(\text{tfa})$ ² (tfa = 1,1,1-trifluoro-2,4-pentanedionate) which extensively decompose on sublimation. The tetrameric *trans*- $[\text{CF}_3\text{CF}=\text{C}(\text{CF}_3)\text{Ag}]_4$ is the only other precursor previously studied. Silver films may be deposited from the organosilver precursor by both plasma-enhanced³ and thermal routes.⁴

The trifluoroacetate and trifluoroacetylacetonate complexes are far from ideal precursors for the CVD of silver films. Excellent precursors should be thermally stable under the sublimation conditions. High vapor pressures are desirable to allow for high deposition rates. Also, the precursor should be a liquid at the vaporization temperature so that the vaporization rate may be easily controlled and not subject to surface area changes associated with the sublimation of solid precursors. Furthermore, the complex should have a clean mechanism for removing the ligands from the metal center so that the growing film may be free from impurities.

We have explored phosphine complexes of silver(I) acetates and acetylacetonates in search of suitable precursors for the deposition of thin

silver films. Metal β -diketonates have long been used in the CVD of metal^{5,6} and metal oxide⁷ films due to their volatility and thermal stability under sublimation conditions. Fluorinated acetylacetonates have proven more volatile than their hydrocarbon analogues and have found extensive use in the CVD of other metals such as copper.⁸⁻¹⁸

Lewis base adducts of copper acetylacetonates have proven excellent precursors for the deposition of copper films.¹⁹⁻²⁴ The great interest in these precursors stems from the disproportionation pathway available to $\text{Cu}(\text{hfac})(\text{L})$ compounds (where $\text{L} = \text{PMe}_3$ or some other Lewis base) which thermally disproportionate to copper metal and the thermally stable $\text{Cu}(\text{hfac})_2$. Thus, clean copper films are produced as the ligands on the precursor atom are cleanly removed by the disproportionation pathway:



The analogous disproportionation of a $\text{Ag}(\text{I})$ precursor is not expected to occur due to an unfavorable redox potential which results from the relative instability of oxygen donor complexes of $\text{Ag}(\text{II})$.²⁵ However, the compounds $\text{Ag}(\text{hfac})(\text{PMe}_3)$ and $\text{Ag}(\text{hfac})(\text{PMe}_3)_2$ undergo redox reactions with other metal surfaces under CVD conditions leading to the controlled, selective deposition of silver on metal substrates.

Several new silver(I) acetato and acetylacetonato trimethylphosphine complexes have been characterized by IR and NMR spectroscopy and X-ray crystallography in order to understand the bonding and factors leading to the volatility of these complexes.

Results and Discussion

Silver(I) acetate complexes. Phosphine adducts of silver carboxylates are well-known and exhibit a variety of stoichiometries. The triphenylphosphine complexes $\text{Ag}(\text{O}_2\text{CR})(\text{PPh}_3)_x$ ($x = 1, 2, \text{ and } 3$)²⁶⁻²⁹ and the dinuclear 1,2-bis(diphenylphosphine)methane and ethane complexes $\text{Ag}_2(\text{O}_2\text{CR})_2(\text{diphos})_x$ ($x = 1 \text{ or } 3$)^{26,29,30} are most common. Rare, however, are the more Lewis basic trialkylphosphine complexes of silver carboxylates.³¹

Trimethylphosphine adducts of silver acetate can be prepared by adding an appropriate amount of phosphine to silver acetate in diethyl ether.



The two complexes are colorless, somewhat air-sensitive solids.

Unfortunately, the acetate complexes are not suitable for the CVD of thin silver films as they decompose under sublimation conditions.

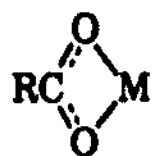
The dinuclear $\text{Ag}_2(\text{OAc})_2(\text{dmpe})$ was prepared by adding one-half an equivalent of dmpe to $\text{Ag}(\text{OAc})$ in dichloromethane giving a colorless, air-stable solid.



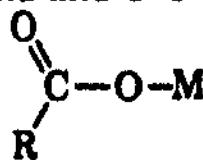
Silver carboxylates are commonly insoluble and light sensitive, and thus little is known about their structures despite their extensive use in the polymerization of urethane. Silver trifluoroacetate³² and perfluorobutyrate,³³ two of the very few silver(I) carboxylates which have been crystallographically characterized, possess dimeric structures with bridging carboxylates. Crystallographic studies of silver carboxylate

phosphine complexes are equally as sparce.^{28,30} However, infrared spectroscopy has been more widely employed to investigate the silver-carboxylate bonding in these complexes.

IR spectroscopic studies. IR spectroscopy has been applied to elucidate the mode of bonding adopted by carboxylato ligands in many metal complexes.³⁴ The difference between the asymmetric and symmetric CO₂ stretching frequencies, which roughly corresponds to $\nu_{C=O}$ and ν_{C-O} , is sensitive to the coordination mode of the carboxylate. The spectra of unidentate carboxylates show an increase in frequency of the CO₂ asymmetric stretch and a similar decrease in the CO₂ symmetric stretch due to localization of the C=O double bond and C-O single bond.



bidentate



unidentate

If the difference $\Delta\nu = \nu_{CO_{asym}} - \nu_{CO_{sym}}$ is approximately equal to the value found in alkali metal salts, the carboxylate is probably bidentate. If $\Delta\nu$ is much larger, the carboxylate is very likely unidentate.

The values of $\Delta\nu$ are summarized in Table I-1. All three new acetato complexes have $\Delta\nu$ values approximately equal to that found in Na(OAc) where $\Delta\nu = 164 \text{ cm}^{-1}$. Therefore the IR data suggest that the acetato groups are bidentate.

However, the above analysis does not distinguish between chelating and bridging acetato groups. A distinction can be made by noting that bridging carboxylates generally have larger O-C-O angles than chelating carboxylates. Gregorev theoretically found that an increase in the O-C-O

Table I-1: Infrared stretching frequencies of the silver(I) acetato phosphine complexes reported in wavenumbers (cm^{-1})

Carboxylate Symmetric and Asymmetric Stretching Frequencies

	$\nu_{\text{CO}_{\text{asym}}}$	$\nu_{\text{CO}_{\text{sym}}}$	$\Delta\nu$
Ag(OAc)(PMe₃)	1570	1420	150
Ag(OAc)(PMe₃)	1565	1430	135
Ag₂(OAc)₂(dmpe)	1575	1380	195
Free carboxylate anion taken as Na(OAc)			164

angle also increases $\Delta\nu$, although not as dramatically as if the carboxylate were unidentate.²⁵ Thus the IR study suggests that the trimethylphosphine complexes $\text{Ag}(\text{OAc})(\text{PMe}_3)$ and $\text{Ag}(\text{OAc})(\text{PMe}_3)_2$ are bidentate acetate groups while $\text{Ag}_2(\text{OAc})_2(\text{dmpe})$ possess acetate ligands which bridge two silver centers.

Silver(I) β -diketonate complexes. Phosphine adducts of silver β -diketonates are much less common than of silver carboxylates. As with the carboxylates, most are triphenylphosphine complexes such as $\text{Ag}(\beta\text{-diketonate})(\text{PPh}_3)_2$.³⁶

Silver(I) acetylacetonato trimethylphosphine complexes can be prepared by addition of a stoichiometric amount of trimethylphosphine to ether suspensions of $\text{Ag}(\text{acac})$ or solutions of $\text{Ag}(\text{hfac})$.



The acetylacetonate complexes are air-sensitive and somewhat light sensitive, while the hexafluoroacetylacetonate complexes are not sensitive to air and light.

Both silver β -diketonates appear to also form tris(trimethylphosphine) complexes, $\text{Ag}(\beta\text{-diketonate})(\text{PMe}_3)_3$, in the presence of excess phosphine as high C, H, and P microanalyses are common after the first crystallization. Furthermore, the $^{31}\text{P}(^1\text{H})$ NMR spectrum of $\text{Ag}(\text{hfac})(\text{PMe}_3)_2$ sublimed from an oil exhibits a weak resonance with a $^1J(^{107}\text{Ag}-\text{P})$ coupling constant of 323 Hz which supports the presence of a trisphosphine impurity. Therefore, it is important to use a stoichiometric or a slightly deficient amount of PMe_3 in the synthesis of the $\text{Ag}(\beta\text{-diketonate})(\text{PMe}_3)_x$ ($x = 1$ or 2) complexes.

Crystallization followed by sublimation yields analytically pure complexes; however, some decomposition invariably occurs upon sublimation limiting the yield of this process. Also, $\text{Ag}(\text{acac})(\text{PMe}_3)_2$ sublimes to give analytically pure $\text{Ag}(\text{acac})(\text{PMe}_3)$.

The structures of silver acetylacetonates are also not well-known, despite their extensive use as NMR shift agents in conjunction with paramagnetic lanthanide acetylacetonate complexes.³⁷⁻³⁹ Additionally, there has been no crystallographic work on silver β -diketonates and their phosphine adducts.

³¹P(¹H) NMR spectroscopic studies. ³¹P(¹H) NMR spectroscopy has proven to be a very powerful tool to understand bonding in silver-phosphine complexes.^{31,40-45} Coupling between the $I=1/2$ nuclear spins of the ¹⁰⁷Ag and ¹⁰⁹Ag nuclei (51.8% and 48.2% natural abundances, respectively) and the ³¹P nucleus results in a ³¹P(¹H) NMR spectrum which consists of two superimposed doublets (Figure 1). Only for chelating diphosphines⁴⁴ or bulky monophosphines,³¹ however, is coupling resolved at room temperature. The greater kinetic lability of smaller unidentate phosphine ligands leads to rapid intermolecular phosphine exchange on the NMR time scale. Cooling to temperatures of -80 °C or lower is often required to resolve ¹J_{Ag-P} coupling.⁴⁰

The ¹J_{Ag-P} coupling constant is dependent on the number of phosphines coordinated to the silver center; ¹J_{Ag-P} decreases upon increasing number of phosphines. For example, in representative the series $\text{Ag}(\text{BF}_4)(\text{PEt}_3)_x$, $J_{\text{Ag-P}} = 712, 482, 304,$ and 218 Hz for $x = 1, 2, 3,$ and $4,$

$${}^1J_{107}^{\text{Ag-P}} = 719.1 \text{ Hz}$$

$${}^1J_{109}^{\text{Ag-P}} = 830.2 \text{ Hz}$$

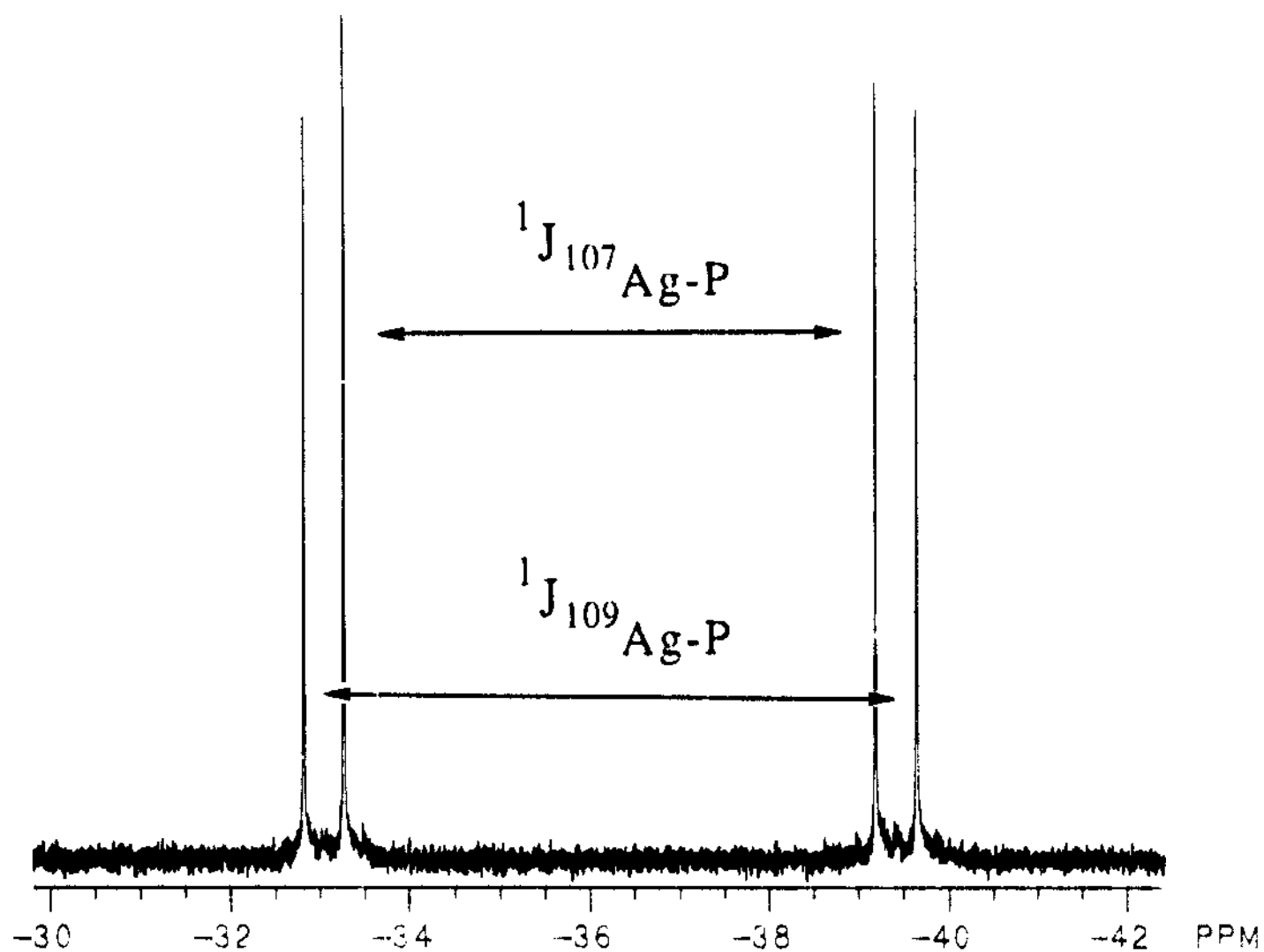


Figure 1: ${}^{31}\text{P}\{^1\text{H}\}$ NMR spectrum of $\text{Ag}(\text{acac})(\text{PMe}_3)$ recorded at 121.6 MHz and $-80\text{ }^\circ\text{C}$

respectively.⁴⁴ Thus, the magnitude of $J_{\text{Ag-P}}$ is diagnostic of the number of phosphines bonded to the silver center.

Comparison of $J_{\text{Ag-P}}$ values in complexes with the same number of phosphines can give more detailed information about the Ag-P bonding. Specifically, the magnitude of $J_{\text{Ag-P}}$ has been correlated with the degree of s-character in the Ag-P bonds.^{40,41} For example, as the P-Ag-P angle in silver bisphosphine complexes increases, the s-character of the Ag-P bond increases, and the Ag-P bonds become more "sp-like". Also, increased s-character in the Ag-P bond may manifest itself in a decreased Ag-P distance. Therefore, comparison of the $J_{\text{Ag-P}}$ coupling constants can yield information on the structure of the P-Ag-P unit in solution.

The $^{31}\text{P}(^1\text{H})$ NMR parameters in d^2 -dichloromethane for the trimethylphosphine adducts are summarized in Table I-2. The coupling constants follow the trend observed for other phosphine adducts; $^1J_{\text{Ag-P}}$ for a monophosphine complex is larger than for the analogous bisphosphine complex. Unfortunately, for $\text{Ag}(\text{OAc})(\text{PMe}_3)_2$ phosphine exchange was rapid at $-90\text{ }^\circ\text{C}$ and $J_{\text{Ag-P}}$ could not be measured.

The largest $J(^{107}\text{Ag-P})$ coupling constant was recorded for $\text{Ag}(\text{hfac})(\text{PMe}_3)$. As expected, this value found in the monophosphine complex is larger than any found in the bisphosphine complexes. Usually $J_{\text{Ag-P}}$ does not change dramatically with the anionic ligand; however, $J(^{107}\text{Ag-P})$ was significantly larger (ca. 50 Hz) than $J(^{107}\text{Ag-P})$ found in the other two analogous complexes $\text{Ag}(\text{acac})(\text{PMe}_3)$ and $\text{Ag}(\text{OAc})(\text{PMe}_3)$. This disparity suggests that there is more s-character in the Ag-P bond of $\text{Ag}(\text{hfac})(\text{PMe}_3)$ which is not surprising since hexafluoroacetylacetonate is

Table I-2: $^{31}\text{P}\{^1\text{H}\}$ NMR parameters of Ag(I) trimethylphosphine complexes recorded at 121.6 MHz and -80 to -90 °C in d^2 -dichloromethane

	δ (ppm)	$^1J(^{107}\text{Ag-P})$ (Hz)
	-----	-----
Ag(OAc)(PMe₃)	-35.2	700
Ag(acac)(PMe₃)	-36.6	719
Ag(hfac)(PMe₃)	-36.4	764
Ag(OAc)(PMe₃)₂	-38.0	*
Ag(acac)(PMe₃)₂	-38.1	445^a
Ag(hfac)(PMe₃)₂	-36.4	507
Ag(OAc)(PPh₃)₂	8.1	421

* Phosphine exchange is too rapid to resolve $J_{\text{Ag-P}}$ coupling as a broad singlet with fwhm = 28 Hz was observed at -90 °C.

a A broad doublet with a peak separation of 445 Hz was observed in which coupling to both ^{107}Ag and ^{109}Ag nuclei was not resolved.

a much weaker base than either acetate or acetylacetonate and should bind more weakly to the metal center.

For comparison, $J(^{107}\text{Ag-P})$ was recorded for $\text{Ag}(\text{OAc})(\text{PPh}_3)_2$ ^{26,27} in order to examine the effects of changing the phosphine in bisphosphine complexes. Although rapid phosphine exchange at $-90\text{ }^\circ\text{C}$ prevents the resolution of $J_{\text{Ag-P}}$ and comparison to the analogous $\text{Ag}(\text{OAc})(\text{PMe}_3)_2$, the other bisphosphine complexes may be compared to $\text{Ag}(\text{OAc})(\text{PPh}_3)_2$ as $J_{\text{Ag-P}}$ generally does not change dramatically with the anionic ligand. The magnitude of the $J_{\text{Ag-P}}$ coupling constant is larger in the bis(trimethylphosphine) complexes than in $\text{Ag}(\text{OAc})(\text{PPh}_3)_2$ which suggests that there is a larger degree of s-character in the Ag-P bond for the PMe_3 adducts. In contrast to a previous study where an increasing value of $J_{\text{Ag-P}}$ was correlated with increasing electronegativity of the groups bonded to phosphorus,⁴⁴ the more electronegative phenyl groups in PPh_3 give a decreased $J_{\text{Ag-P}}$ coupling constant. The related acetylacetonato trimethylphosphine complexes show $J_{\text{Ag-P}}$ coupling constants on the order of 100 Hz larger. The greater Lewis basicity of PMe_3 thus leads to a stronger interaction with the silver center and greater s-character in the Ag-P bonds as compared to the less Lewis basic PPh_3 . As a result, the Ag-P bonds in the PMe_3 complexes should be shorter and the P-Ag-P angles should be larger than in analogous PPh_3 complexes.

The $^{31}\text{P}(^1\text{H})$ NMR spectra are very solvent dependent. No distinct coupling between $^{107}\text{Ag-P}$ and $^{109}\text{Ag-P}$ nuclei can be resolved in d^8 -toluene; however, in some cases an estimate of $J_{\text{Ag-P}}$ can be made from the separation between two broad doublets. For example, $J_{\text{Ag-P}} = 748\text{ Hz}$ for

$\text{Ag}(\text{acac})(\text{PMe}_3)_2$ in d^8 -toluene at $-80\text{ }^\circ\text{C}$. Somewhat surprisingly, a value near 700 Hz suggests that this species is a monophosphine complex. However, free PMe_3 was not observed at -63 ppm .

In light of the interesting Ag-P interactions which the $^{31}\text{P}\{^1\text{H}\}$ NMR studies suggest, single crystal X-ray crystallographic studies were performed on three representative complexes to further elucidate the bonding in these complexes.

X-Ray Crystallographic studies. Single crystals of $\text{Ag}(\text{OAc})(\text{PMe}_3)_2$ were obtained by allowing a warm, saturated pentane solution to cool to room temperature overnight. Selected crystallographic data and bond distances and angles are given in Tables II-3 and II-4.

Consistent with the IR data, molecules of $\text{Ag}(\text{OAc})(\text{PMe}_3)_2$ are monomeric and have chelating acetato ligands (Figure 2). The related copper complex $\text{Cu}(\text{OAc})(\text{PPh}_3)_2$ is also monomeric.⁴⁶

Surprisingly, the Ag-O distances of 2.476 (2) and 2.542 (2) Å are longer than the Ag-P distances of 2.3985 (7) and 2.4047 (6) Å. The Ag-O distances are longer than found in the few structurally characterized silver carboxylates where distances of 2.23-2.24 Å were found in the dimeric $[\text{Ag}(\text{O}_2\text{CCF}_3)]_2$ ³² and $[\text{Ag}(\text{O}_2\text{CC}_3\text{F}_7)]_2$.³³ One of two silver acetate phosphine complexes previously crystallographically characterized is the tetrameric $[\text{Ag}(\text{OAc})(\text{PPh}_3)]_4$ which has Ag-O bond distances of 2.23 - 2.32 Å for oxygens bound to one silver center and 2.475 Å for an oxygen bridging two silver centers.²⁸ A broader range of Ag-O distances of 2.25 - 2.63 Å was found in the bis(1,8-naphthalenedicarboxylato) complex with a Ag_4O_8 core $[(\text{C}_{12}\text{H}_6\text{O}_4)(\text{Ph}_3\text{PAg})_4]$.³⁰ Long Ag-O distances of 2.54 to 2.85 Å have been

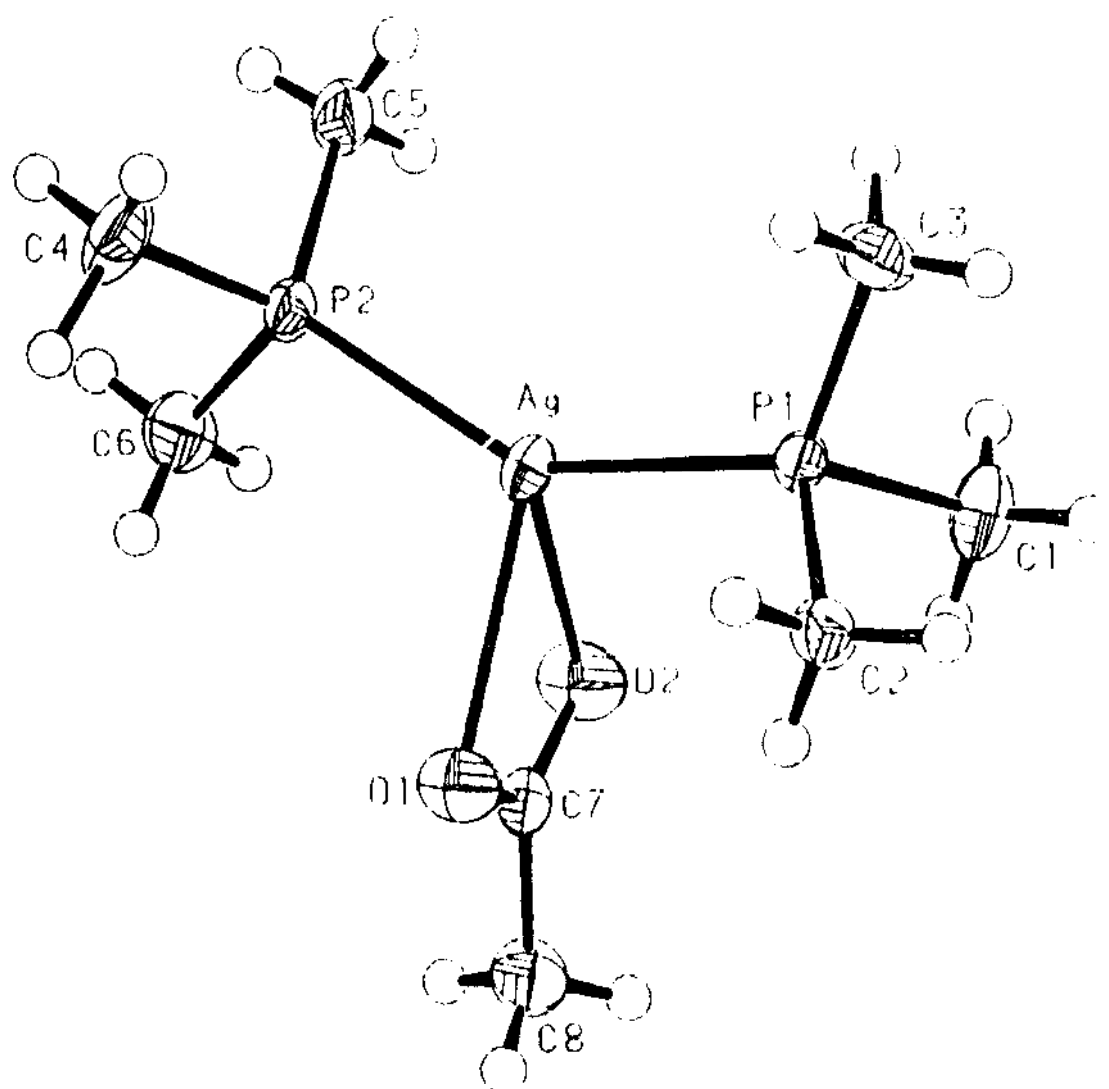


Figure 2: ORTEP representation of $\text{Ag}(\text{OAc})(\text{PMe}_3)_2$ in which thermal ellipsoids are shown at the 35 % probability level

Table I-3: Selected crystallographic data for $\text{Ag}(\text{OAc})(\text{PMe}_3)_2$

Space group:	$P2_1/c$	Temp:	-75 °C
a:	10.222 (3) Å	β :	105.65 (2)°
b:	10.095 (1) Å	V:	1427 (1) Å ³
c:	14.321 (3) Å	Z:	4
R ^a :	0.021	R _w ^b :	0.024
λ Mo(K α):	0.71073 Å		

$$^a R = \sum ||F_o| - |F_c|| / \sum |F_o|$$

$$^b R_w = (\sum w(|F_o| - |F_c|)^2 / \sum w|F_o|^2)^{1/2}$$

Table I-4: Selected bond distances and angles in $\text{Ag}(\text{OAc})(\text{PMe}_3)_2$ Bond Distances (Å)

Ag-P1	2.4047 (6)	Ag-P2	2.3985 (7)
Ag-O1	2.476 (2)	Ag-O2	2.542 (2)

Bond Angles (deg)

P1-Ag-P2	147.36 (2)	O1-Ag-O2	51.75 (7)
P1-Ag-O1	103.38 (5)	P2-Ag-O2	102.99 (5)
P1-Ag-O2	102.21 (5)	P2-Ag-O1	109.15 (5)

found in the *o*-allylphenyldimethylarsine adduct

$\text{Ag}(\text{NO}_3)(\text{As}(\text{C}_6\text{H}_4\text{CH}=\text{CH}_2)\text{Me}_2)$ where the nitrate ligand acts as a bridging, doubly bidentate ligand between silver centers.⁴⁷ Thus, long Ag-O bond distances found in other complexes may be attributed to bridging ligands; however, this is not the case in the *monomeric* $\text{Ag}(\text{OAc})(\text{PMe}_3)_2$.

The Ag-P bond distances are similar to many other *monophosphine* silver(I) phosphine complexes. For example, the Ag-P distances of 2.390 (2) Å in $[\text{AgCl}(\text{PEt}_3)]_4$,⁴⁸ 2.402 (5) Å in $[\text{AgBr}(\text{PEt}_3)]_4$,⁴⁸ and 2.415 (5) and 2.429 (2) Å in $[\text{AgBr}(\text{PPh}_3)]_4$ ⁴⁹ compare well to those found in $\text{Ag}(\text{OAc})(\text{PMe}_3)_2$ of 2.4047 (6) and 2.3985 (7) Å. However, the Ag-P distances in $\text{Ag}(\text{OAc})(\text{PMe}_3)_2$ are shorter than found in other *bisphosphine* adducts, which possess dimeric structures. In $[\text{AgCl}(\text{PPh}_3)_2]_2$ ⁵¹ and $[\text{AgBr}(\text{PPh}_3)_2]_2 \cdot \text{CHCl}_3$ ⁵² the Ag-P bond distances are longer, ranging from 2.47 to 2.51 Å.

The P-Ag-P angle of 147.36 (2)° of $\text{Ag}(\text{OAc})(\text{PMe}_3)_2$ deviates significantly from the idealized tetrahedral angle of 109.47°. In a related monomeric copper complex, $\text{Cu}(\text{OAc})(\text{PPh}_3)_2$,⁴⁶ the P-Cu-P angle of 133.4 (1)° is also larger than 109.5°, but this can be attributed to steric effects. The relatively large PPh_3 ligand is able to reduce interphosphine steric interactions by opening the P-Cu-P angle without unfavorable interactions from the smaller acetato ligand. In contrast, $\text{Ag}(\text{OAc})(\text{PMe}_3)_2$ has smaller phosphines and a larger metal center, both of which reduce steric repulsions. Thus the large P-Ag-P angle must result from electronic effects reflecting an increased degree of s-character in the Ag-P bond. Therefore, the Ag center may be considered as having an "sp-like" hybridization. The shortened Ag-P bond distances found in

$\text{Ag}(\text{OAc})(\text{PMe}_3)_2$ as compared to other bisphosphine adducts also reflect the greater participation of the phosphines in s-type bonds to metal center.

Molecular Structures of $\text{Ag}(\text{hfac})(\text{PMe}_3)$ and $\text{Ag}(\text{hfac})(\text{PMe}_3)_2$.

Suitable crystals of $\text{Ag}(\text{hfac})(\text{PMe}_3)$ and $\text{Ag}(\text{hfac})(\text{PMe}_3)_2$ were grown from pentane solutions at $-20\text{ }^\circ\text{C}$. The preliminary structures are reported as the models have not yet converged during refinement. Selected crystallographic data and bond distance and angles appear in Tables II-5 - II-8.

In contrast to a proposed polymeric structure for $\text{Ag}(\text{acac})$,³⁸ both $\text{Ag}(\text{hfac})(\text{PMe}_3)$ and $\text{Ag}(\text{hfac})(\text{PMe}_3)_2$ are monomeric with no significant Ag-Ag contacts. However, there are large differences between the two structures which result from the coordinated phosphines.

Molecules of $\text{Ag}(\text{hfac})(\text{PMe}_3)$ have planar three coordinate Ag centers that lay in the plane of the phosphorus atom of PMe_3 and the oxygen atoms of the β -diketonate ligand. There are three independent molecules in the unit cell, one of which is shown in Figure 3. The bond distances and angles of the other molecules are similar to that of molecule 1; however, the other two molecules show disorder in the orientation of the CF_3 groups of the β -diketonate ligand. The structure of $\text{Ag}(\text{hfac})(\text{PMe}_3)$ is very closely related to that of the analogous Cu(I) complex $\text{Cu}(\text{hfac})(\text{PMe}_3)$.^{52,53}

The Ag-O bond distances of 2.28 (1) and 2.30 (1) Å reveal that within experimental error, the hexafluoroacetylacetonate ligand is bound to the silver center in a symmetrically chelating manner. The Ag-O distances are not unusual for an oxygen atom bound to one silver center. The O-Ag-O angle of 80.2 (4)^o shows a substantially smaller bite angle of the chelate than

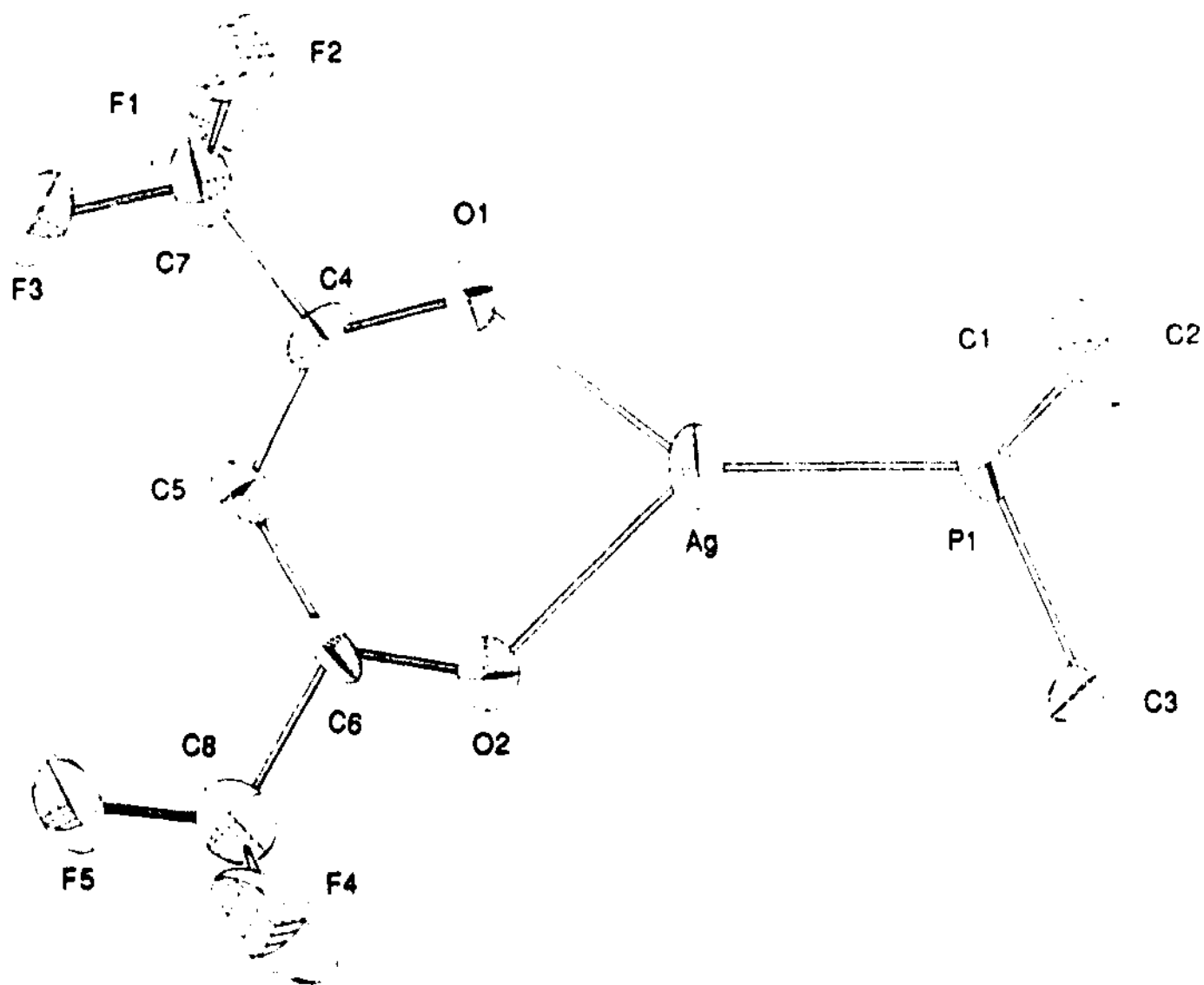


Figure 3: ORTEP representation of $\text{Ag}(\text{hfac})(\text{PMe}_3)$ in which thermal ellipsoids are shown at the 35 % probability level. Hydrogen atoms have not been located in this incompletely refined structure.

Table I-5: Selected crystallographic data for Ag(hfac)(PMe₃)

Space group:	P $\bar{1}$	Temp:	-75 °C
a:	10.911 (3) Å	α :	94.92 (2) ^o
b:	12.536 (3) Å	β :	102.56 (2) ^o
c:	14.937 (3) Å	γ :	94.71 (2) ^o
V:	1976 (12) Å ³	Z:	6
R ^a :	0.068	R _w ^b :	0.064
λ Mo(K α):	0.71073 Å		

$$^a R = \Sigma ||F_o| - |F_c|| / \Sigma |F_o|$$

$$^b R_w = (\Sigma w(|F_o| - |F_c|)^2 / \Sigma w |F_o|^2)^{1/2}$$

Table I-6: Selected bond distances and angles for molecule 1 of Ag(hfac)(PMe₃)

<u>Bond Distances (Å)</u>		<u>Bond Angles (deg)</u>	
Ag-P	2.313 (5)	O1-Ag-O2	80.2 (4)
Ag-O1	2.28 (2)	P-Ag-O1	143.1 (3)
Ag-O2	2.30 (2)	P-Ag-O2	136.7 (3)

the value of $91.9(2)^\circ$ reported for $\text{Cu}(\text{hfac})(\text{PMe}_3)$. The decrease in the bite angle may be attributed to the longer Ag-O bond distances as a consequence of the larger radius of the Ag center.

The Ag-P bond distance of $2.313(5) \text{ \AA}$ found in $\text{Ag}(\text{hfac})(\text{PMe}_3)$ is the shortest reported Ag-phosphine bond. Other short Ag-P bonds to triphenylphosphine are in the range of $2.35 - 2.40 \text{ \AA}$.^{30,54} As suggested with the large value of 757 Hz for $J(^{107}\text{Ag}-\text{P})$, a large degree of s-character in the Ag-P bond results in a decrease in bond length. The strong Lewis basicity of PMe_3 combined with its small size thus leads to a very strong interaction between PMe_3 and the silver center.

The molecular structure of $\text{Ag}(\text{hfac})(\text{PMe}_3)_2$ consists of an asymmetric four-coordinate Ag center which is shown in Figures 4 and 5. Comparison of the P-Ag-O angles shows that the plane of the hexafluoroacetylacetonate ligand is twisted from perpendicular to the P-Ag-P plane. There is a large disparity between the two Ag-O distances. The Ag-O1 distance is $2.45(2) \text{ \AA}$ while the Ag-O2 distance of $2.64(2) \text{ \AA}$ is ca. 0.2 \AA longer. The Ag-O distances in $\text{Ag}(\text{hfac})(\text{PMe}_3)_2$ are ca. 0.15 to 0.35 \AA longer than in the mono(trimethylphosphine) complex $\text{Ag}(\text{hfac})(\text{PMe}_3)$, but in the same range as those found in $\text{Ag}(\text{OAc})(\text{PMe}_3)_2$ ($2.47 - 2.54 \text{ \AA}$). The asymmetrical nature of the chelating hexafluoroacetylacetonate ligand may result from the large Lewis basicity of the PMe_3 donors. The silver center becomes more electronically saturated by the PMe_3 donors in the bisphosphine complexes, which leads to an electron-rich center and a softer electronic potential about its coordination environment. Anionic ligands consequently interact less strongly with the silver center, and the softer

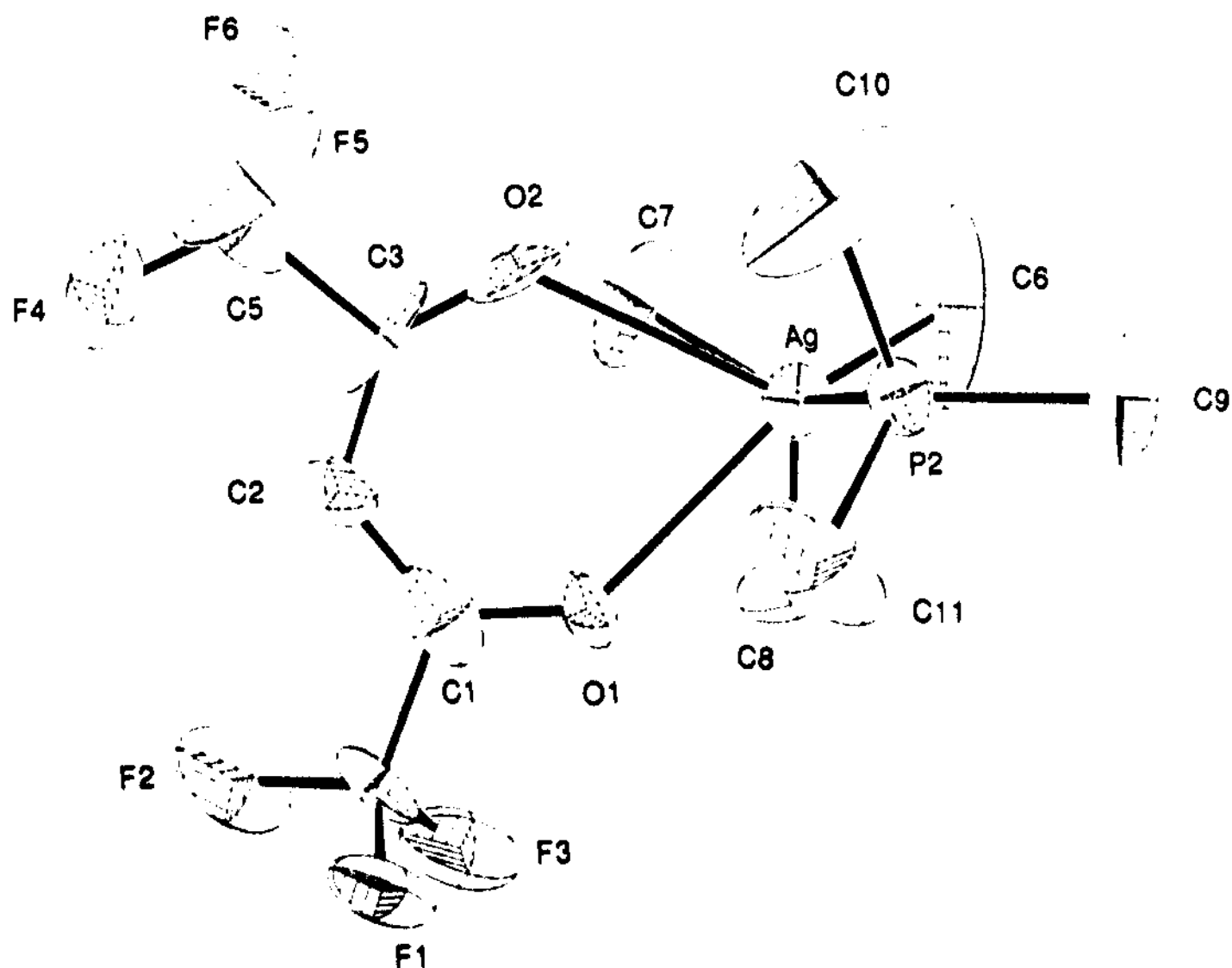


Figure 4: ORTEP representation of $\text{Ag}(\text{hfac})(\text{PMe}_3)_2$ viewed down the Ag-P1 bond showing the asymmetrical nature of the chelate. Thermal ellipsoids are shown at the 35 % probability level. Hydrogen atoms have not been located in this incompletely refined structure.

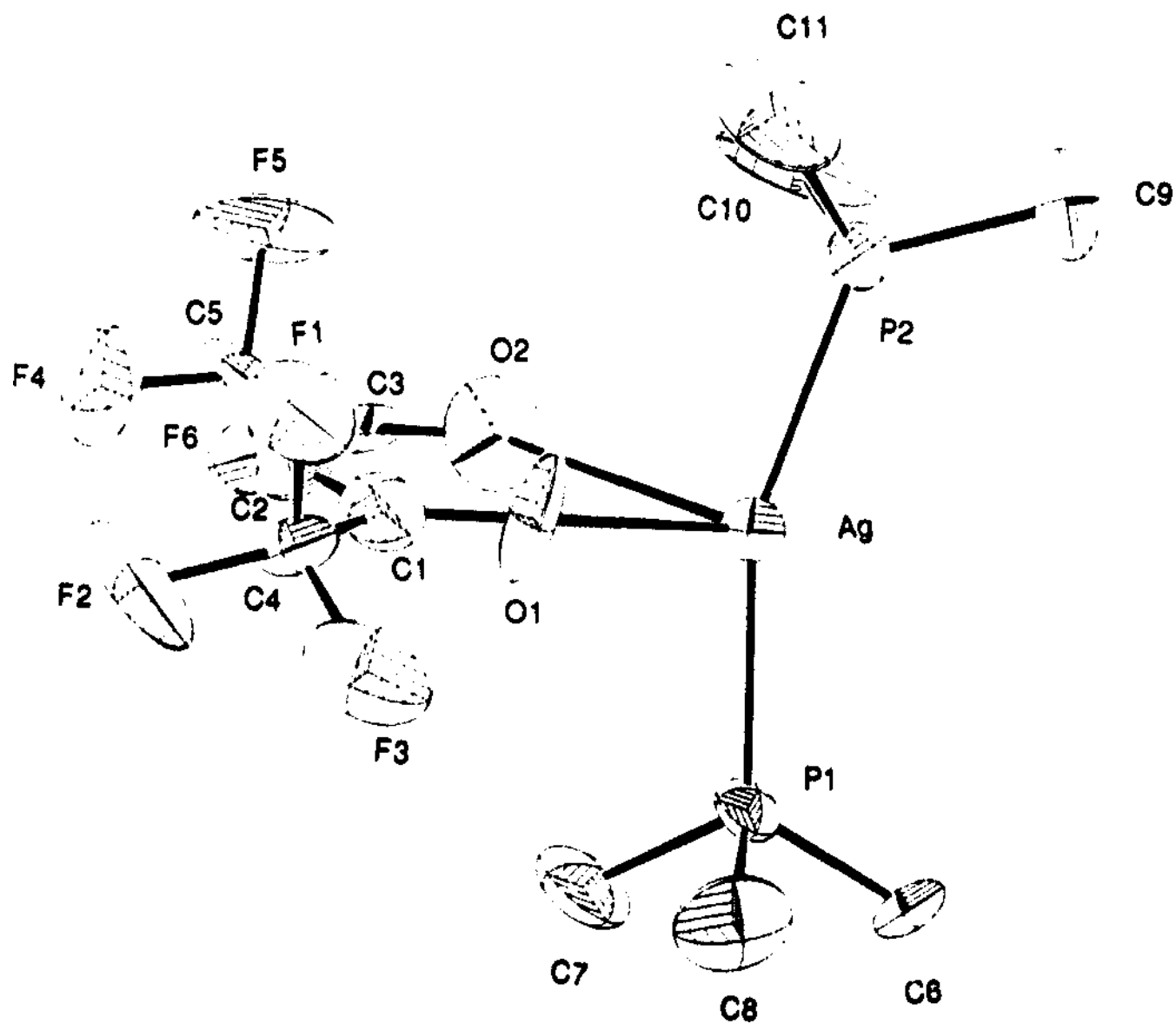


Figure 5: ORTEP representation of $\text{Ag}(\text{hfac})(\text{PMe}_3)_2$ viewed in the P1-Ag-P2 plane highlighting the large P-Ag-P bond angle.

Table I-7: Selected crystallographic data for Ag(hfac)(PMe₃)₂

Space group:	Ia	Temp:	-75 °C
a:	12.315 (5) Å	β:	104.19 (4)°
b:	9.111 (7) Å	V:	11887 (10) Å ³
c:	17.347 (7) Å	Z:	4
R ^a :	0.051	R _w ^b :	0.052
λ Mo(K _α):	0.71073 Å		

$$^a R = \sum ||F_o| - |F_c|| / \sum |F_o|$$

$$^b R_w = (\sum w(|F_o| - |F_c|)^2 / \sum w|F_o|^2)^{1/2}$$

Table I-8: Selected bond distances and angles in Ag(hfac)(PMe₃)₂Bond Distances (Å)

Ag-P1	2.335 (9)	Ag-P2	2.417 (9)
Ag-O1	2.45 (2)	Ag-O2	2.64 (2)

Bond Angles (deg)

P1-Ag-P2	159.4 (2)	O1-Ag-O2	70.3 (7)
P1-Ag-O1	91.3 (7)	P2-Ag-O2	91.6 (6)
P1-Ag-O2	106.9 (6)	P2-Ag-O1	103.8 (7)

potential results in a decrease in preference for a symmetrically chelating mode of bonding.

In addition to the asymmetrical Ag-O bonds, the Ag-P distances are also inequivalent. The Ag-P1 distance of 2.335 (9) Å is almost 0.1 Å shorter than the Ag-P2 distance of 2.417 (9) Å. While the Ag-P1 distance is the second shortest Ag-P bond to a phosphine, the Ag-P2 distance falls within the normal range of Ag-P distances and is very similar to the average Ag-P distance found in Ag(OAc)(PMe₃)₂ of 2.40 Å. Though the difference of ca. 0.08 Å in Ag-P bond distances is chemically significant, there does not appear to be any chemical reason for the inequivalence. The P-Ag-P angle of 159.4 (4)° is also much larger than the idealized tetrahedral angle of 109.47° and is much larger than the P-Cu-P angle of 127.10 (6) found in Cu(hfac)(PPh₃)₂⁵⁵ and is similar to the P-Ag-P angle of 147° found in Ag(OAc)(PMe₃)₂.

The short Ag-P distances and large P-Ag-P angle suggests that the Ag-P bonds are "sp-like" and that the solid state structure of Ag(hfac)(PMe₃)₂ approaches that of a linear [Me₃P-Ag-PMe₃]⁺ cation with a weakly associated hexafluoroacetylacetonate anion. Further support of the ion pair nature of the solid state structure is that Ag(hfac)(PMe₃)₂ is a 1:1 conductor in methanol.

Conclusion

The synthesis of acetato and acetylacetonatosilver(I) trimethylphosphine complexes is straightforward. IR spectroscopy shows the acetato ligands are chelating in the trimethylphosphine complexes and

bridging in $\text{Ag}_2(\text{OAc})_2(\text{dmpe})$. $^{31}\text{P}(^1\text{H})$ NMR spectroscopy suggests a large degree of s-character in the Ag-P bond of the PMe_3 complexes. X-ray crystallographic studies further substantiate the large interaction between the Ag centers and the very Lewis basic PMe_3 ligands as shown by the two shortest reported Ag-phosphine distances along with P-Ag-P angles of 147° and 159° in the bis(trimethylphosphine) complexes.

The strongly Lewis basic PMe_3 ligands electronically saturate the silver center resulting in volatile, monomeric complexes. By forming short Ag-P distances and large P-Ag-P angles, trimethylphosphine controls the coordination around the Ag center and leads to long Ag-anion distances in the bis(trimethylphosphine) complexes.

Experimental

All operations were carried out in vacuum or under argon except where noted. Pentane and diethyl ether were distilled under nitrogen from sodium benzophenone and toluene from sodium immediately before use. Methanol was distilled under nitrogen from magnesium ethoxide prepared from iodine activated magnesium. Trimethylphosphine⁵⁶ and 1,2-bis(dimethylphosphino)ethane were prepared from literature routes.⁵⁷ Silver(I) acetylacetonate was prepared by a literature procedure while silver hexafluoroacetylacetonate was prepared by a modified literature route.³⁸ Silver acetate was purified by recrystallization from a hot solution of 20% acetic acid. Silver nitrate was used as received.

The IR spectra were recorded on a Perkin-Elmer 599B infrared spectrometer as Nujol mulls. The ^1H NMR data were obtained on Varian

XL-200, General Electric QE-300, or General Electric GN-300NB spectrometers. ^{31}P NMR spectra were recorded on a General Electric GN-300NB at 121.6 MHz. All chemical shifts are reported in δ -units relative to TMS (^1H) or 85% H_3PO_4 (^{31}P). Microanalyses were performed by the University of Illinois Microanalytical Laboratory and the mass spectra were recorded by the University of Illinois Mass Spectrometry Laboratory. The crystal structure determinations were performed by Dr. Scott Wilson and Ms. Teresa Pruszk-Wieckowski of the University of Illinois X-ray Crystallographic Laboratory.

(Trimethylphosphine)acetatosilver(I) To a suspension of $\text{Ag}(\text{OAc})$ (0.68 g, 4.1 mmol) in ether (65 mL) in a foil-covered flask was added by syringe PMe_3 (0.41 mL, 4.1 mmol). After the mixture had been stirred for 2 h, the $\text{Ag}(\text{OAc})$ was consumed giving a yellow solution and black residue. The solution was filtered and concentrated to ca. 15 mL. Cooling to $-20\text{ }^\circ\text{C}$ yielded off-white needles. Yield: 0.45g (45%). Mp. $76\text{-}76.5\text{ }^\circ\text{C}$. Anal. Calcd: C, 33.95; H, 5.70. Found: C, 34.15; H, 5.71. IR (cm^{-1}): 1570 s, 1420 m, 1330 m, 1282 m, 1260 w, 1000 w, 962 s, 945 m sh, 911 m, 750 w, 745 w, 795 w br, 741 m, 660 m, 640 w, 609 w. ^1H NMR (C_6D_6): δ 2.47 (s, O_2CH_3), 0.25 (d, PMe_3 , $J_{\text{PH}} = 8.2\text{ Hz}$). $^{31}\text{P}\{^1\text{H}\}$ NMR (CD_2Cl_2 , $-80\text{ }^\circ\text{C}$): δ -35.2 (d, $J(^{107}\text{Ag-P}) = 700\text{ Hz}$).

Bis(trimethylphosphine)acetatosilver(I) To a suspension of $\text{Ag}(\text{OAc})$ (0.98g, 5.87 mmol) in ether (60 mL) was added by syringe PMe_3 (1.8 mL, 18 mmol). After the solution had been stirred for 5 minutes, all of the $\text{Ag}(\text{OAc})$ had dissolved. The solution was stirred overnight. The solution was removed in vacuum and the residue was extracted into ether (10 mL). The filtered extract was cooled to $-20\text{ }^\circ\text{C}$ to yield clear crystals. The crystals

were washed with a small amount of pentane and dried in vacuo. Yield: 0.97 g (52%). Mp. 50.5 - 51.5 °C. Anal. Calcd: C, 30.12; H, 6.63. Found: C, 30.01; H, 6.60. IR (cm⁻¹): 1565 s, 1430 m, 1414 m, 1392 m br, 1326 m, 1301 w, 1283 m, 960 s, 949 s sh, 910 m, 854 w, 732 m, 666 w, 645 m, 613 w. ¹H NMR (C₆D₆): δ 2.53 (s, O₂CH₃), 0.85 (d, PMe₃, J_{PH} = 6.0 Hz). ³¹P{¹H} NMR (CD₂Cl₂, -90 °C): δ -38.0 (s, fwhm = 28 Hz).

μ-1,2-bis(dimethylphosphinoethane)bis(acetato)disilver(I) To a suspension of Ag(OAc) (0.65g, 3.89 mmol) in dichloromethane (50 mL) in a foil-covered flask was added by syringe dmpe (0.32 mL, 1.9 mmol). After the solution had been stirred for 2 h, all of the Ag(OAc) was consumed giving a yellow solution and a black residue. The solution was filtered, concentrated to ca. 5 mL., and cooled to -20 °C to afford off-white columnar crystals. Yield: 0.47g (50%). Anal. Calcd: C, 24.82; H, 4.58; P, 13.22; Ag, 44.58. Found: C, 24.83; H, 4.63; P, 13.40; Ag, 44.74. IR (cm⁻¹): 1478 vs, 1435 s, 1400 m sh, 1332 s, 1301 m, 1288 w, 1194 m, 1122 m, 1108 w, 958 s, 920 m, 902 m, 884 w, 858 w, 818 vw, 747 m, 735 m, 659 m, 617 w. ¹H NMR (C₆D₆): δ 2.14 (s br, O₂CH₃), 1.91 (d, PCH₂), 1.46 (t, PCH₃). ³¹P{¹H} NMR (CD₂Cl₂, -80 °C): δ -26.7 (s, fwhm 16.7 Hz).

(Trimethylphosphine)acetylacetonatosilver(I) To a suspension of Ag(acac) (0.89 g, 4.3 mmol) in ether (120 mL) in a foil-covered flask was added PMe₃ (0.9 mL, 8.9 mmol). After the mixture had been stirred for 2 h, the solvent was removed in vacuum and the residue remained in vacuum for 2 h. The residue was extracted in to pentane (4 x 80 mL) and concentrated to ca. 175 mL. Cooling to -20 °C afforded white needles. Yield: 0.13 g (12%). Anal. Calcd.: C, 33.95; H, 5.70. Found: C, 34.15; H, 5.71. IR

(cm^{-1}): 1590 vs, 1559 s, 1505 s, 1436 s, 1398 s br, 1308 vw, 1294 m, 1261, w, 1235 m, 1195 m, 1010 m, 960 s, 945 m sh, 914 m, 847 w, 784 m, 738 m, 676 w, 650 m, 536 m, 407 m. ^1H NMR (CD_2Cl_2): δ 5.50 (s, CH), 2.00 (s, CH_3), 1.60 (d, PMe_3 , $J_{\text{PH}} = 7.95$ Hz). $^{31}\text{P}\{^1\text{H}\}$ NMR (CD_2Cl_2 , -80 °C): δ -36.6 ($^1J(^{107}\text{Ag}-\text{P}) = 719$ Hz).

Bis(trimethylphosphine)acetylacetonatosilver(I) To a suspension of $\text{Ag}(\text{acac})$ (1.66 g, 8.02 mmol) in pentane (300 mL) in a foil-covered flask was added PMe_3 (1.65 mL, 16.1 mmol). The mixture was stirred for 16 h. Additional pentane (80 mL) was added, and the solution was filtered, concentrated to ca. 150 mL, and cooled to -20 °C to afford clear crystals. A second crop of crystals was obtained by concentration of the resulting supernatant and cooling to -20 °C. Yield: 1.75 g (61%). Anal. Calcd: C, 36.79; H, 7.02. Found: C, 37.49; H, 7.28. IR (cm^{-1}): 1604 s, 1508 s, 1410 s br, 1290 m sh, 1280 m, 1225 m, 1195 w, 1156 w, 1000 m, 947 s, 901 m, 842 w, 790 w, 753 m, 728 m, 681 m, 649 w, 612 w, 520 m, 404 m. ^1H NMR (C_6D_6): δ 5.42 (s, CH), 2.18 (s, CCH_3), 0.89, (d, PMe_3 , 5.1 Hz). $^{31}\text{P}\{^1\text{H}\}$ NMR (C_7D_8 , -87 °C): δ -37.4 (d, $J_{\text{AgP}} = 748$ Hz, coupling to ^{107}Ag and ^{109}Ag centers was not resolved). $^{31}\text{P}\{^1\text{H}\}$ NMR (CD_2Cl_2 , -90 °C): δ -38.1 (d br, $J_{\text{AgP}} = 445$ Hz, coupling to ^{107}Ag and ^{109}Ag centers was not resolved).

Hexafluoroacetylacetonatosilver(I) This procedure was performed in air as $\text{Ag}(\text{hfac})$ is not air-sensitive. A $\text{Na}(\text{hfac})$ solution was prepared by adding 1,1,1,5,5,5-2,4-pentanedione (hfacH) (4.4 mL, 31 mmol) to a solution of NaOH (1.22 g, 30.4 mmol) in water (10 mL). The pH was adjusted with a few drops of hfacH so that the pH was less than 4. The $\text{Na}(\text{hfac})$ solution was added to a solution of $\text{Ag}(\text{NO}_3)$ (5.17 g, 30.4 mmol) in 10 mL of water in

a foil-covered flask. The resulting solution was stirred for 10 min. The aqueous solution was extracted with ether (4 x 60 mL). The ether layer was separated, filtered, and dried over Na_2SO_4 . After the solvent was removed in vacuum, the solid was extracted into methanol (40 mL). The extract was filtered, concentrated, and cooled to $-20\text{ }^\circ\text{C}$ to afford clear crystals. Yield: 2.45 g (26%). Anal. Calcd: C, 19.07; H, 0.32. Found: C, 19.90; H, 0.53. IR (cm^{-1}): 1664 s, 1644 s, 1608 w, 1556 s, 1534 s, 1320 w br, 1263 s, 1204 s br, 1255 s sh, 1235 vs br, 1181 m, 934 w, 800 m, 781 m, 739 m, 730 w sh, 665 s, 587 m, 527 w.

(Trimethylphosphine)hexafluoroacetylacetonatosilver(I) To a solution of $\text{Ag}(\text{hfac})$ (0.99 g, 3.1 mmol) in ether (20 mL) was added PMe_3 (0.32 mL, 3.1 mmol). After the solution had stirred for 4 h, the solvent was removed under vacuum. The white product was sublimed at 10^{-4} Torr and $80\text{ }^\circ\text{C}$ onto a water-cooled cold finger for 8 h. Yield: 0.94 g (76%). Anal. Calcd: C, 24.51; H, 2.57. Found: C, 24.61; H, 2.68. IR (cm^{-1}): 1670 s, 1545 m sh, 1530 s, 1435 w, 1424 m, 1365 w sh, 1310 w, 1291 m, 1250 s, 1285 s br, 1135 s br, 1070 m, 952 m, 938 m sh, 847 w, 782 m, 750 m sh, 735 m, 659 s, 577 m, 524 w, 420 w, 385 w, 376 w. ^1H NMR (C_7D_8): δ 6.32 (s, CH), 0.30 (d, PMe_3 , $J_{\text{PH}} = 8.2\text{ Hz}$). $^{31}\text{P}(^1\text{H})$ NMR (CD_2Cl_2 , $-87\text{ }^\circ\text{C}$): δ -36.4 (d, $J(^{107}\text{Ag}-\text{P}) = 764\text{ Hz}$). M.S. (10 eV, m/e): 390, 15%, $[\text{Ag}(\text{hfac})(\text{PMe}_3)]^+$; 230, 7%; 183, 79%, $[\text{Ag}(\text{PMe}_3)]^+$; 139, 10%, $[\text{CF}_3\text{COCH}_2\text{CO}]^+$; 76, 100%, $[\text{PMe}_3]^+$; 61, 54%, $[\text{PMe}_2]^+$.

Bis(trimethylphosphine)hexafluoroacetylacetonatosilver(I)

Method 1: To a solution of $\text{Ag}(\text{hfac})$ (0.68 g, 2.2 mmol) in ether (40 mL) was added PMe_3 (0.4 mL, 3.9 mmol). After the solution had been stirred for 2 h, the solvent was removed in vacuum and the residue was extracted into

pentane (2 x 70 mL). The solution was concentrated to ca. 50 mL when a small amount clear granules began to precipitate. The solution was cooled to -20 °C to afford more granular precipitate. The solution was filtered, concentrated to ca. 10 mL, and cooled to -20 °C to afford clear crystals. Yield: 0.80 g (80%). Anal. Calcd: C, 28.29; H, 4.10. Found: C, 28.93; H, 5.01. The crystals may be sublimed to afford an analytically pure sample. Mp. 69.5 - 70 °C. Anal. Found: C, 28.31; H, 4.10. Λ (10^{-3} M in MeOH, 25 °C) = $94 \Omega^{-1} \text{ cm}^2 \text{ M}^{-1}$. IR (cm^{-1}): 1670 s, 1598 w, 1552 s, 1527 s, 1423 m, 1304 w sh, 1289 m, 1248 s, 1189 s sh, 1178 s, 1145 vs br, 1059 w sh, 962 m, 944 s, 843 vw, 782 m, 745 w br, 730 m, 655 s, 573 m, 521 w. $^1\text{H NMR}(\text{C}_6\text{D}_6)$: δ 6.27 (s, CH), 0.73 (d, PMe_3 , $J_{\text{PH}} = 6.7$ Hz). $^{31}\text{P}\{^1\text{H}\}$ NMR (CD_2Cl_2 , -87 °C): δ -36.4 (d, $J(^{107}\text{Ag}-\text{P}) = 507$ Hz). MS (10 eV, m/e): 390, 2%, $[\text{Ag}(\text{hfac})(\text{PMe}_3)]^+$; 259, 20%, $[\text{Ag}(\text{PMe}_3)_2]^+$; 183, 14%, $[\text{Ag}(\text{PMe}_3)]^+$; 139, 3%, $[\text{CF}_3\text{COCH}_2\text{CO}]^+$; 76, 100%, $[\text{PMe}_3]^+$; 61, 54%, $[\text{PMe}_2]^+$.

Method 2: To a solution of $\text{Ag}(\text{hfac})$ (0.67 g, 2.1 mmol) in ether (15 mL) was added PMe_3 (0.45 mL, 4.4 mmol). After the solution had been stirred for 2 h, the solvent was removed in vacuum to give a clear oil. The white product was sublimed from the oil at 10^{-4} Torr and 60 °C onto a water-cooled cold finger for 8 h. Yield: 0.38 g (38%). Calcd: C, 28.29; H, 4.10. Found: C, 29.33; H, 4.55.

References

1. Anon. *Res. Discl.* 1986, 263, 146.
2. Anon. *Res. Discl.* 1986, 261, 61.
3. Oehr, C.; Suhr, H. *Appl. Phys. A* 1989, 49, 691-696.
4. Jeffries, P. M.; Girolami, G. S. submitted to *Chem. Mater.*
5. Van Hemer, R. L.; Spendlove, L. B.; Sievers, R. E. *J. Electrochem. Soc.* 1965, 112, 1123-1126.
6. Moshier, R. W.; Sievers, R. E.; Spendlove, L. B. U.S. Patent 3 356 527, 1967.
7. Bridge, S. I.; Dunhill, N. I.; Williams, J. O. *Chemtronics* 1989, 4, 266.
8. Lecohier, B.; Philippoz, J. M.; Calpini, B.; Stumm, T.; Van Den Bergh, H. *J. de Physique IV* 1991, 1, C2-279-C2-286.
9. Kaloyeros, A. E.; Feng, A.; Garhart, J.; Brooks, K. C.; Ghosh, S. K.; Saxena, A. N.; Luehrs, F. *J. Elect. Mater.* 1990, 19, 271-276.
10. Temple, D.; Reisman, A. *J. Electrochem. Soc.* 1989, 136, 3525-3529.
11. Armitage, D. N.; Dunhill, N. I.; West, R. H.; Williams, J. O. *J. Cryst. Growth* 1991, 108, 683-687.
12. Pilkington, R. D.; Jones, P. A.; Ahmed, W.; Tomlinson, R. D.; Hill, A. E.; Smith, J. J.; Nuttall, R. *J. de Physique IV* 1991, 1, C2-263-C2-269.
13. Kaloyeros, A. E.; Saxena, A. N.; Brooks, K. C.; Ghosh, S. K.; Eisenbraun, E. *Mat. Res. Soc. Symp. Proc.* 1990, 181, 79-85.
14. Oehr, C.; Suhr, H. *Appl. Phys. A* 1988, 45, 151-154.
15. Houle, F. A.; Wilson, R. J.; Baum, T. H. *J. Vac. Sci. Technol. A* 1968, 4, 2452-2458.

16. Houle, F. A.; Jones, C. R.; Baum, T. H.; Pico, C.; Kovac, C. A. *Appl. Phys. Lett.* 1985, **46**, 204-206.
17. Moylan, C. R.; Baum, T. H.; Jones, C. R. *Appl. Phys. A* 1986, **40**, 1-5.
18. Markwalder, B.; Widmer, M.; Braichotte, D.; Van Der Bergh, H. *J. Appl. Phys.* 1989, **65**, 2470-2474.
19. Norman, J. A. T.; Muratore, B. A.; Dyer, P. N.; Roberts, D. A.; Hochberg, A. K. *J. de Physique IV* 1991, **1**, C2-271-C2-278.
20. Shin, H. K.; Chi, K. M.; Hampden-Smith, M. J.; Kostas, T. T.; Farr, J. D.; Paffett, M. *Adv. Mater.* 1991, **3**, 246-248.
21. Kumar, R.; Fronczek, F. R.; Maverick, A. W.; Lai, W. G.; Griffin, G. L. *Chem. Mater.*, submitted.
22. Chi, K. M.; Shin, H. K.; Hampden-Smith, M. J.; Duesler, E. N.; Kostas, T. T. *Polyhedron* 1991, **10**, 2293-2299.
23. Reynolds, S. K.; Smart, C. J.; Baran, E. F.; Baum, T. H.; Larson, C. E.; Brock, P. J. *Appl. Phys. Lett.* 1991, **59**, 2332-2334.
24. Chi, K. M.; Shin, H. K.; Hampden-Smith, M. J.; Kostas, T. T.; Duesler, E. N. *Inorg. Chem.* 1991, **30**, 4293-4294.
25. Lancashire, R. J. In *Comprehensive Coordination Chemistry*; Wilkinson, G.; Gillard, R. D.; McCleverty, J. A., Eds.; Pergamon Press: Oxford, 1987, pp 844-845.
26. Edwards, D. A.; Longly, M. J. *Inorg. Nucl. Chem.* 1978, **40**, 1599.
27. Oldham, C.; Sanford, W. F. *J. Chem. Soc., Dalton Trans.* 1977, 2068-2070.
28. Blues, E. T.; Drew, M. G. B.; Femi-Onadeko, B. *Acta Cryst.* 1977, **B33**, 3965-3967.

29. van der Ploeg, A. F. M. J.; van Koten, G. *Inorg. Chim. Acta* 1981, 51, 225-239.
30. van der Ploeg, A. F. M. J.; van Koten, G.; Spek, A. L. *Inorg. Chem.* 1979, 18, 1052.
31. Geol, R. G.; Pilon, P. *Inorg. Chem.* 1978, 17, 2876-2879.
32. Griffin, R. G.; Ellet, J. D. Jr.; Mehring, M.; Bullitt, J. G.; Waughm J. *S. J. Chem. Phys.* 1972, 57, 2147.
33. Blakeslee, A. E.; Hoard, J. L. *J. Am. Chem. Soc.* 1965, 78, 3029.
34. Mehrota, R. C.; Bohra, R. *Metal Carboxylates*; Academic Press: London, 1983, pp 51-54.
35. Gregorev, A. I. *Russ. J. Inorg. Chem.* 1963, 8, 409.
36. Gibson, D.; Johnson, B. F. C.; Lewis, J. *J. Chem Soc. (A)* 1970, 367-369.
37. Wenzel, T. J.; Bettes, T. C.; Sadlowski, J. E.; Sievers, R. E. *J. Am. Chem. Soc.* 1980, 102, 5903.
38. Wenzel, T. J.; Sievers, R. E. *Anal. Chem.* 1981, 53, 393.
39. Wenzel, T. J.; Sievers, R. E. *J. Am. Chem. Soc.* 1982, 104, 382-388.
40. Muetterties, E. L.; Alegranti, C. W. *J. Am. Chem. Soc.* 1972, 94, 6386.
41. Hollander, F. J.; Ip, Y. L.; Coucouvanis, D. *Inorg. Chem.* 1976, 15, 2230.
42. Alyea, E. C.; Dias, S. A.; Stevens, S. *Inorg. Chim. Acta* 1980, 44, L203.
43. Price, S. J. B.; Brevard, C.; Pagleot, A.; Sadler, P. J. *Inorg. Chem.* 1985, 24, 4278.
44. Socol, S. M.; Verkade, J. G. *Inorg. Chem.* 1984, 23, 3487.
45. Barron, P. F.; Dyason, J. C.; Healy, P. C.; Engelhardt, L. M.; Skelton, B. W.; White, A. H. *J. Am. Chem. Soc., Dalton Trans.* 1986, 1965.

46. Drew, M. G. B.; Othman, A. H. B. *Acta Cryst.* 1975, *B31*, 2965-2967.
47. Cooper, M. K.; Nyholm, R. S.; Carreck, P. W.; McPartlin, M. *J. Chem. Soc., Chem. Commun.* 1974, 343.
48. Malatesta, L.; Naldini, L. Simonetta, G.; Cariatì, F. *Coord. Chem. Rev.* 1966, *1*, 255.
49. Uson, R.; Royo, P.; Laguna, A.; Garcia, J. *Rev. Acad. Cienc. Exactas, Fis-Quim. Nat. Zaragoza* 1973, *28*, 67.
50. Howatson, J.; Morosin, B. *Cryst. Struct. Commun.* 1973, *2*, 51.
51. Teo, B. K.; Calabrese, J. C. *J. Chem. Soc., Chem. Commun.* 1976, 185.
52. Shin, H. K.; Hampden-Smith, M. J.; Kostas, T. T.; Duesler, E. N. *Polyhedron* 1991, *6*, 645.
53. Shin, H. K.; Chi, K. M.; Farkas, J.; Hampden-Smith, M. J.; Kostas, T. T.; Duesler, E. N. *Inorg. Chem.* 1992, *31*, 424-431.
54. Teo, B. K.; Calabrese, J. C. *Inorg. Chem.* 1976, *15*, 2467.
55. Bartlett, M. W. Ph. D. Thesis, University of Waterloo, 1970.
56. Luetkins, M. L.; Sattleberger, A. P.; Murray, H. H.; Basil, J. D.; Fackler, J. P. *Inorg. Synth.* 1989, *26*, 7-12.
57. Henderson, R. A.; Hussain, W.; Leigh, G. J.; Normanton, F. B. *Inorg. Synth.* 1985, *23*, 141-143.

Chapter 2

Selective Chemical Vapor Deposition of Silver Films by Transmetalization Reactions

Introduction

The selective deposition of metals by chemical vapor deposition is a topic of great current interest, and is particularly relevant to the metallization of microelectronic devices.¹ Especially important is the selective deposition of Cu films on metallic vs. insulating surfaces. Recently it has been discovered that $\text{Cu}(\text{hfac})(\text{L})$ complexes (where $\text{L} = \text{PMe}_3$, vinyltrimethylsilane, or some other Lewis base) are sometimes able to deposit copper selectively.²⁻⁶ Though the exact origin of selectivity remains unknown, studies suggest that Lewis bases can coordinate to metal surfaces and influence the reactivity of surface-bound intermediates.⁷

General routes for the selective deposition of metal films by CVD may be possible if the precursor undergoes a specific chemical reaction only with certain surfaces. In a few cases, "transmetalation" reactions are known in which metal atoms from the precursor replace atoms in the substrate. For example, under high vacuum and high temperatures, metal halide vapors undergo surface transmetalation reactions with reactive metals, resulting in the deposition of the precursor metal and removal of the surface metal as its halide.⁸ Selective deposition of thin W and Ag films on silicon results from reaction of WF_6 and AgF with Si surfaces under CVD conditions producing the volatile byproduct SiF_4 .^{9,10} Though the reaction of metal halides with metal or Si surfaces may be

general,⁹ the low volatility of most metal halides renders this route to selective deposition of limited use. A similar transmetallation reaction has been suggested as one of several pathways in the CVD of aluminum alkyls on silicon surfaces.¹¹

Metal-organic precursors offer a substantial increase in volatility over their metal halide counterparts; however, reports of selective deposition using volatile metal-organic precursors are sparse. Furthermore, there have been few reports of the CVD of silver films from metal-organic precursors, and none of these addresses the issue of selectivity.¹²⁻¹⁵ The selective deposition of Ag films from metal-organic precursors on Cu, Fe, and Zn surfaces under CVD conditions is here reported where the metal surface plays a much more involved role: the surface reduces the metal-organic precursors in a redox transmetallation reaction to give new metal-organic byproducts that contain atoms that were formerly in the surface.

Results and Discussion

Deposition of Ag on Cu surfaces from $\text{Ag}(\text{hfac})(\text{PMe}_3)$ and $\text{Ag}(\text{hfac})(\text{PMe}_3)_2$. The selective chemical vapor deposition of thin Ag films on copper surfaces from $\text{Ag}(\text{hfac})(\text{PMe}_3)$ and $\text{Ag}(\text{hfac})(\text{PMe}_3)_2$ complexes can be achieved at 10^{-4} Torr and 275 - 350 °C. No deposition occurs on glass, silicon, nickel, cobalt, or aluminum substrates under the same conditions.

Auger electron spectroscopy after brief sputtering establishes that the films are free from C and O contaminants after brief sputtering. Auger depth-profiling studies reveal that both precursors deposit similar Ag films

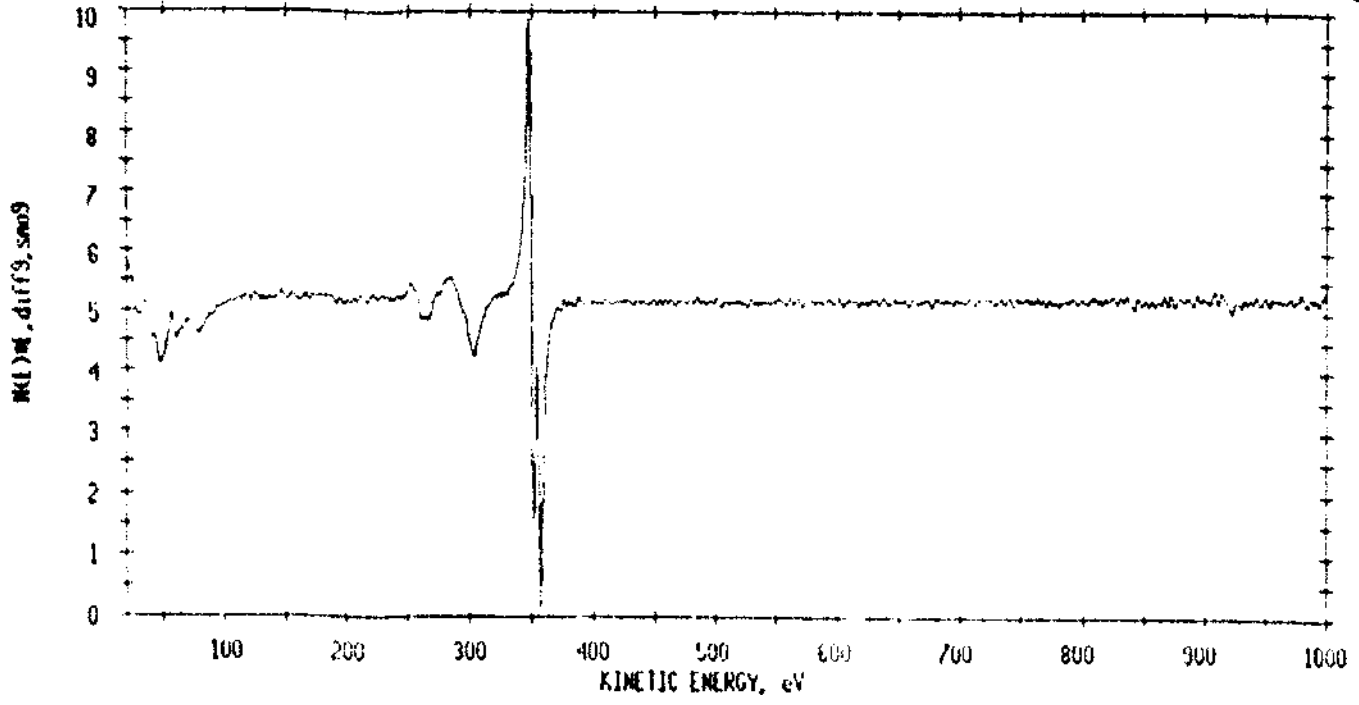


Figure 1a: Auger electron spectrum after brief sputtering of Ag film on Cu deposited from Ag(hfac)(PMe₃) at 275 °C

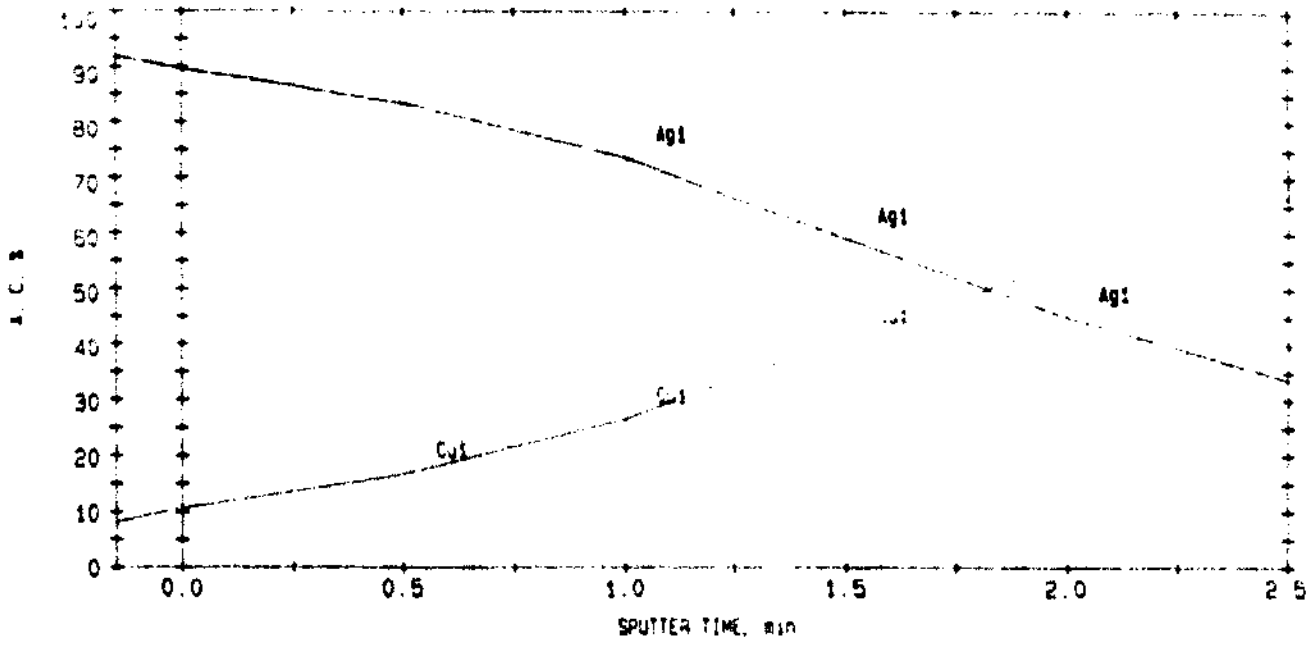


Figure 1b: Auger depth profile with a sputtering rate of ca. 100 Å/min after previous sputtering for 2.5 minutes

on Cu; the Ag concentration decreases from 90% at the surface to 10% at a depth of ca. 1 μm (Figure 1). Although we have no definitive evidence that the films are Ag/Cu alloys, grain boundary interdiffusion¹⁶ may be rapid enough under the reaction conditions to allow for significant diffusion of Ag atoms into the Cu metal substrate.

Scanning electron microscopy reveals that the films deposited on amorphous copper coated silicon substrates are granular. Grains of 0.5 μm and from 0.1 - 0.2 μm in length cover most of the amorphous Cu substrate (Figure 2). Also apparent are larger islands up to 15 μm across consisting of very closely packed grains 0.5 μm grains. The islands are partly surrounded by areas where deposition has not occurred. Thus, the islands may be nucleation sites in which the deposition preferentially occurs. However, the elemental composition of any of the granular or island features has not yet been established by focusing the Auger electron beam on the small area of interest. The grains may be polycrystalline, but X-ray diffraction studies have not yet been performed to establish their crystallinity.

Along with unreacted precursor, a green material condensed on the cool walls of the reaction vessel downstream of the deposition zone. This green material was identified by mass spectrometry as $\text{Cu}(\text{hfac})_2$.¹⁷ Elemental analysis also confirms the presence of Cu in the green byproduct. The precursors therefore undergo a redox reaction with the copper surface that results in the deposition of metal along with generation of the volatile byproduct $\text{Cu}(\text{hfac})_2$, which decomposes readily only above 310 $^\circ\text{C}$ under CVD conditions.

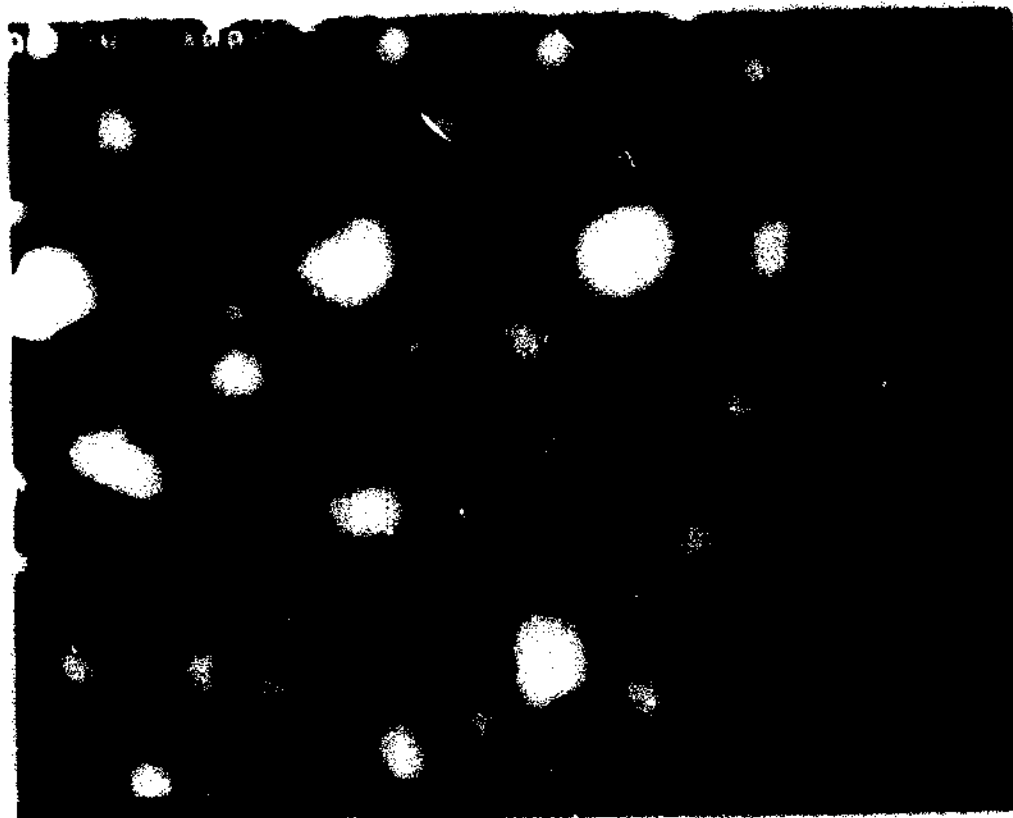


Figure 2a: Scanning electron micrograph obtained at 20 kV of the Ag film on amorphous Cu showing grains of 0.5 and 0.1 - 0.2 μm

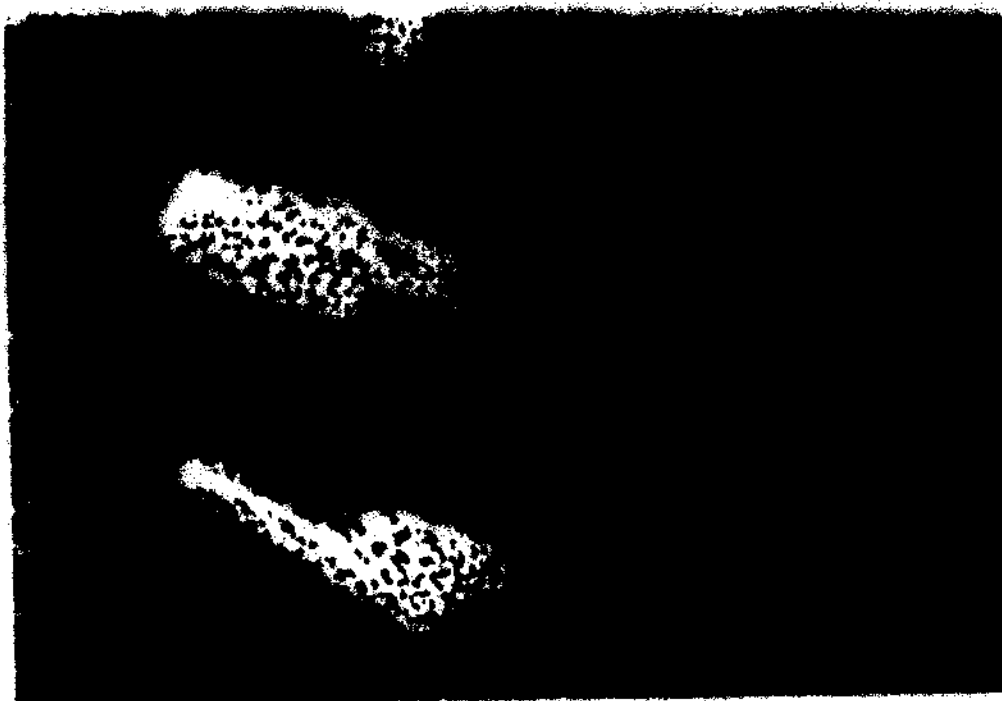


Figure 2b: Island features of ca. 15 μm of Ag film partially surrounded by granular area

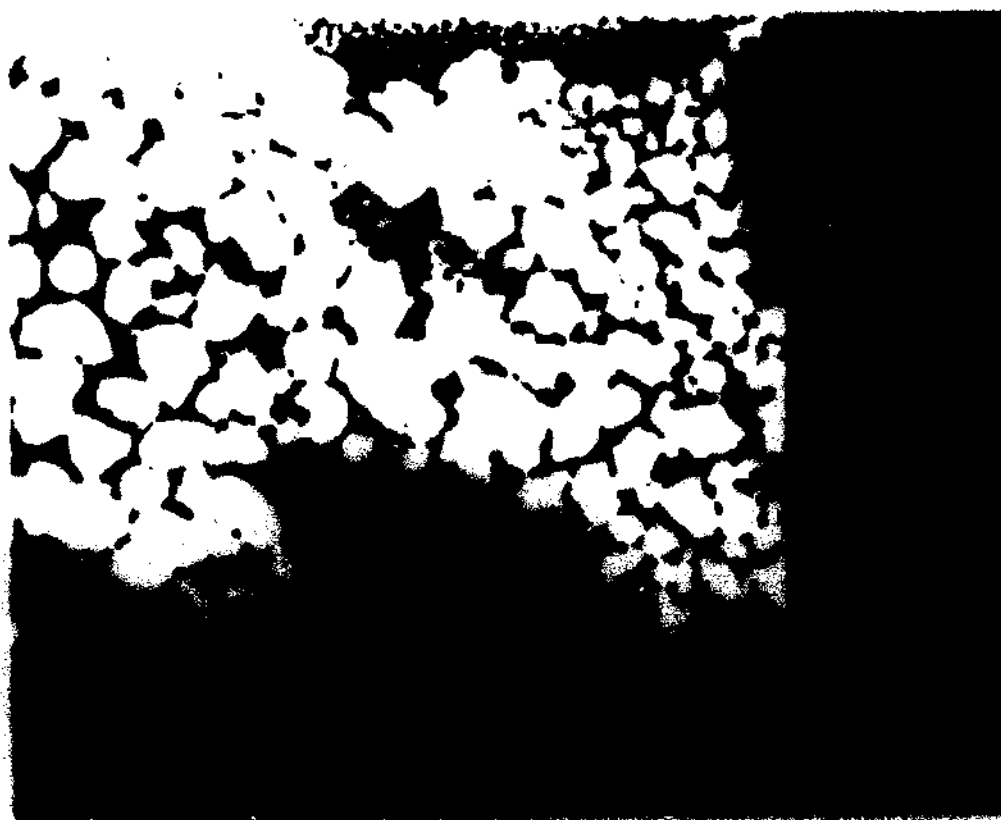


Figure 2c: Magnification of island feature showing it to consist of small grains



There are at least two pathways by which $\text{Ag}(\text{hfac})(\text{PMe}_3)$ and $\text{Ag}(\text{hfac})(\text{PMe}_3)_2$ can react with a copper surface to produce $\text{Cu}(\text{hfac})_2$. The first route is reaction of $\text{Ag}(\text{hfac})(\text{PMe}_3)$ with the Cu surface to yield surface bound Ag atoms and hfac and PMe_3 molecules. The hfac molecules may then migrate to one Cu atom to form $\text{Cu}(\text{hfac})_2$ which leaves the surface. An alternative pathway involves the formation of Ag atoms and a Cu(I) intermediate, $\text{Cu}(\text{hfac})(\text{PMe}_3)$, by reaction of $\text{Ag}(\text{hfac})(\text{PMe}_3)$ with a surface Cu atom. $\text{Cu}(\text{hfac})(\text{PMe}_3)$ may then disproportionate to Cu and $\text{Cu}(\text{hfac})_2$, which is known to occur under CVD conditions above 150 °C.¹⁸ Though analysis of the reaction products cannot distinguish between the two pathways, the appearance of $\text{Cu}(\text{hfac})(\text{PMe}_3)$ in the byproduct mixture suggests that the Cu(I) intermediate pathway accounts for part of the observed formation of $\text{Cu}(\text{hfac})_2$.

Although the intimate mechanism of deposition is not known, the basic reason for selective deposition of Ag on Cu is clear. The thermal stability of $\text{Ag}(\text{hfac})(\text{PMe}_3)$ and $\text{Ag}(\text{hfac})(\text{PMe}_3)_2$ prevents decomposition of the precursor which could result in a impure Ag deposit. The precursors are sufficiently reactive towards the copper surface which insures a Ag deposit. The stability of $\text{Cu}(\text{hfac})_2$ insures that the Cu atom will be removed from the surface with no decomposition of the Cu species.

Deposition of Ag on Fe surfaces from $\text{Ag}(\text{hfac})(\text{PMe}_3)_2$. The selective chemical vapor deposition of thin Ag films on iron substrates from $\text{Ag}(\text{hfac})(\text{PMe}_3)_2$ occurs at 10^{-4} Torr and 275 - 350 °C. No deposition occurs on glass or silicon substrates present under the same conditions.

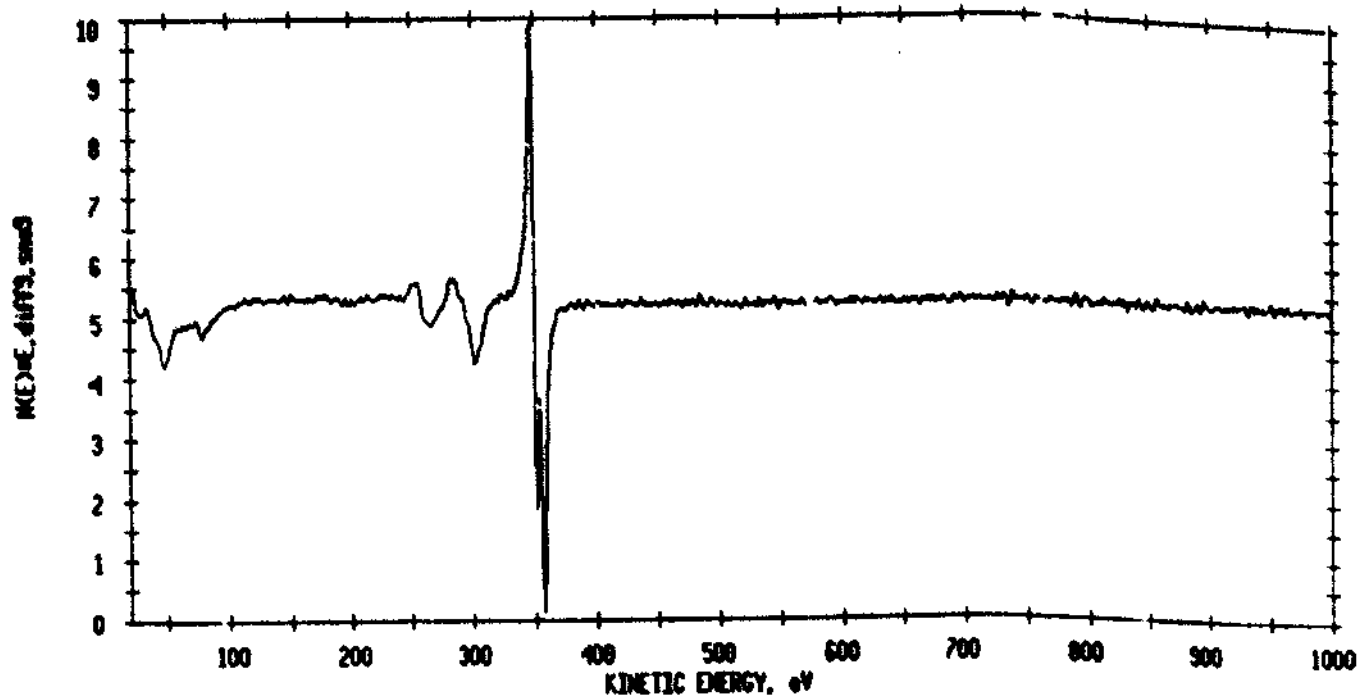


Figure 3a: Auger electron spectrum after brief sputtering of Ag film on Fe deposited from $\text{Ag}(\text{hfac})(\text{PMe}_3)_2$ at 275 °C

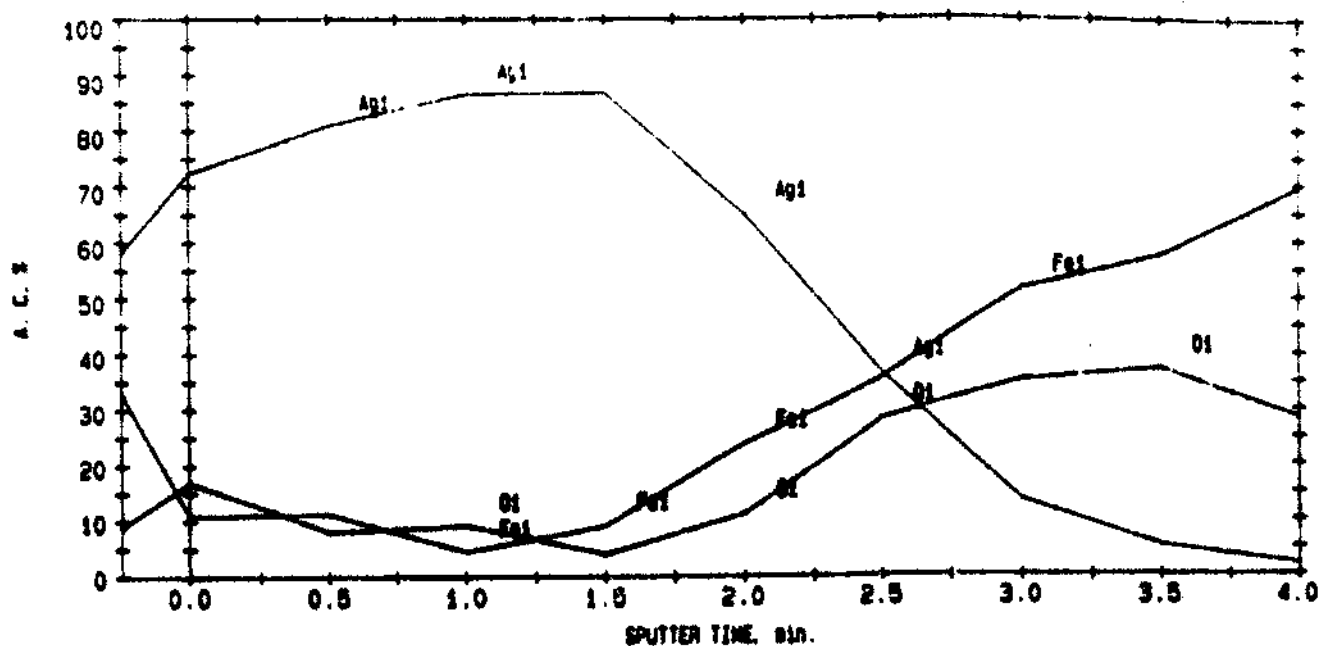


Figure 3b: Auger depth profile with a sputtering rate of ca. 170 Å/min

Auger electron spectroscopy after brief sputtering establishes that the films are free from C and O contaminants (Figure 3). However, Auger depth-profiling studies show a marked increase in Fe and O concentration below a depth of ca. 250 Å. The absence of O contamination on the surface suggests that the O is due to the oxide layer found on Fe surfaces rather than a result of precursor decomposition.

The thermodynamic iron containing product is $\text{Fe}(\text{hfac})_3$ if the deposition proceeds by a transmetallation pathway since the possible Fe(II) product, $\text{Fe}(\text{hfac})_2$, has only been isolated as a dihydrate which decomposes upon heating.¹⁹ Analysis of the light violet byproduct which condensed on the cool walls of the reaction vessel downstream of the deposition zone by mass spectrometry shows peaks at 470 and 401 m/e. The parent ion for $\text{Fe}(\text{hfac})_3$ is not observed in its mass spectrum. Rather, a signal at 470 m/e for $[\text{Fe}(\text{hfac})_2]^+$ is the highest mass seen for $\text{Fe}(\text{hfac})_3$.²⁰ The signal at 401 m/e results from the loss of a CF_3 group from $[\text{Fe}(\text{hfac})_2]^+$. Elemental analysis also confirms the presence of Fe in the byproducts. The selective deposition of Ag on Fe surfaces therefore results from the transmetallation reaction:



The oxygen contamination observed in the film does not appear to come from the Ag precursor because the O concentration is correlated with the Fe concentration. Thus, the transmetallization reaction must be both very efficient and energetically favored for deposition to occur onto the highly oxidized surface.

Deposition of Ag on Zn surfaces from $\text{Ag}(\text{hfac})(\text{PMe}_3)_2$. The chemical vapor deposition of thin Ag films on Zn substrates occurs selectively at 10^{-4} Torr and 200°C in the presence of glass and silicon. After brief sputtering to remove surface contamination, Auger spectroscopy shows the Ag concentration of the film to be 20% (Figure 4). Depth profiling studies show the concentration slowly decreases to 5% at a depth of ca. $0.6 \mu\text{m}$.

The Auger spectra also indicate a significant degree of oxygen contamination in the film. In contrast with the deposition on Fe, there is a sizable amount of oxygen present after brief sputtering. The concentration of oxygen, however, does not increase with increasing concentration of zinc. Though the purity substrate used was not established, further studies are needed to determine the origin of the oxide contamination.

The mass spectrum of the CVD byproducts which condensed on the cool walls of the reactor shows a weak signal at 478 m/e which is attributed to the parent ion of $\text{Zn}(\text{hfac})_2$.²¹ The most intense peak at 409 m/e results from the loss of CF_3 from $\text{Zn}(\text{hfac})_2$. Elemental analysis confirms the presence of 0.36 % Zn in the residue. Therefore, selective deposition of Ag on Zn occurs by a transmetallation reaction between the Ag precursor and the Zn substrate.



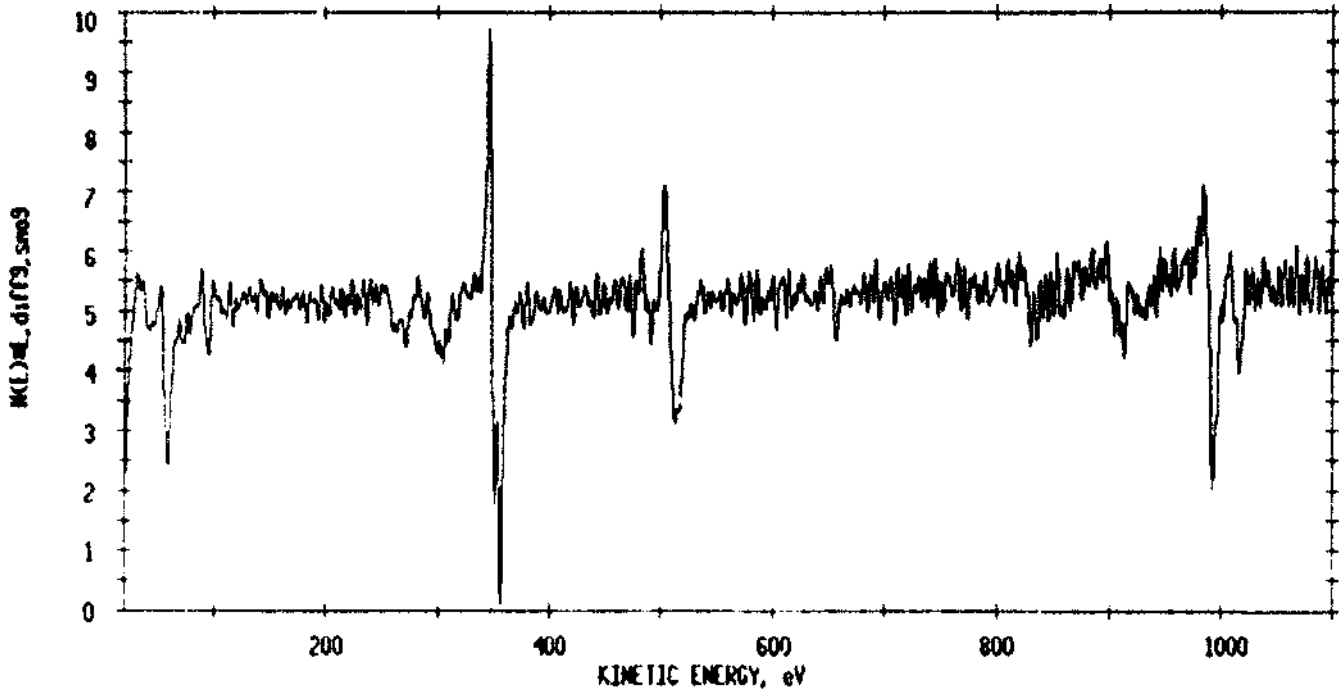


Figure 4a: Auger electron spectrum after brief sputtering of Ag film on Zn deposited from $\text{Ag}(\text{hfac})(\text{PMe}_3)_2$ at 200 °C

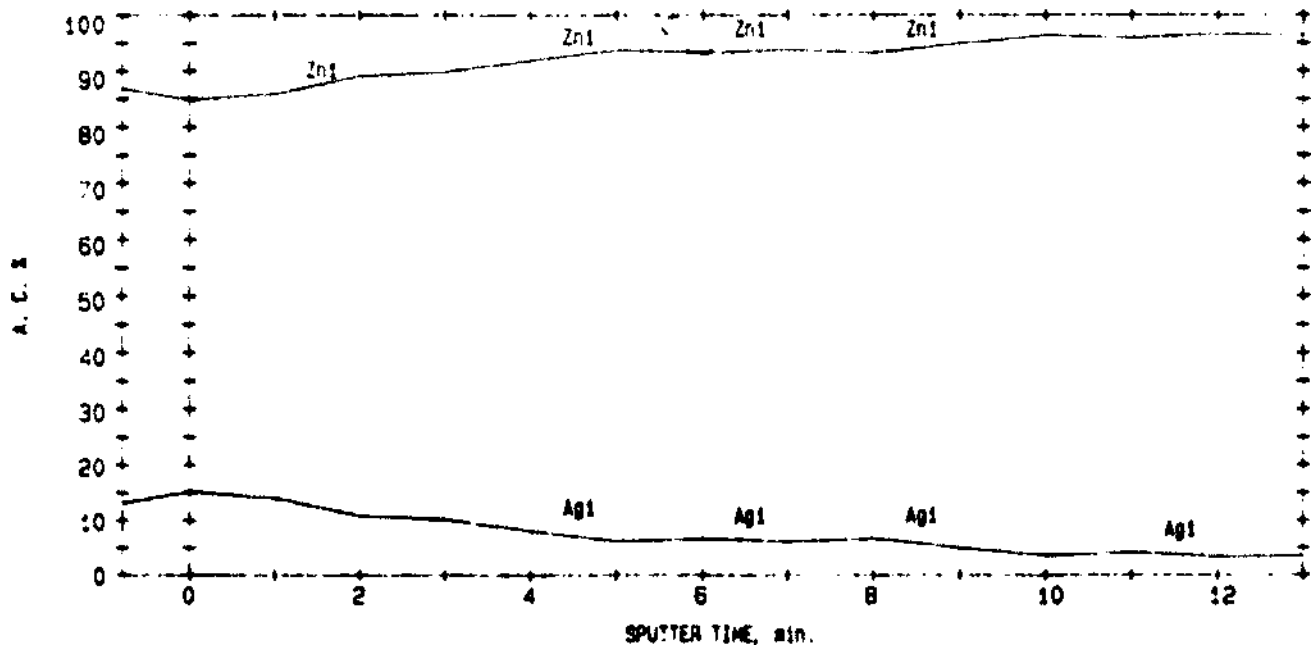


Figure 4b: Auger depth profile with a sputtering rate of ca. 170 Å/min after previous sputtering for 6 minutes at ca. 560 Å/min

Conclusions

For the first time, the selective chemical vapor deposition of metal films from volatile metal-organic precursors has been achieved where the factors controlling the selectivity are clear. A *predictable* redox reaction occurs on the metal substrate which results in reduction of the precursor to deposited metal atoms accompanied by the oxidation of surface atoms to stable, volatile molecules which are removed from the surface. Factors important in predicting selectivity appear only to depend on the existence of a favorable redox potential between the precursor and the metal substrate along with the degree of surface oxidation of the metal substrate. However, the presence of an oxidized surface does not inhibit transmetalization on Fe substrates, which suggests that the reaction is both very energetically favorable and efficient.

Although the CVD of thin Cu films from Lewis base adducts of hexafluoroacetylacetonatecopper(I) complexes is relatively well-developed,^{2-7,18} before these films can be useful in microelectronic devices, the corrosion resistance and electromigration effects must be improved.²³ A thin protective coating of a noble metal may be deposited on the surface of a Cu film if grain boundary diffusion of deposited metal atoms into the substrate is slow. Generally, however, grain boundary interdiffusion may be rapid enough under transmetalization conditions to allow for significant diffusion of deposit and substrate atoms which results in a thin alloy and improved electromigration resistance. Films better suited for

48
microelectronic devices may be obtained by the selective deposition of other metals on or into the Cu film.

The stability and volatility of many metal hexafluoroacetylacetonates may allow us to extend this method to the selective deposition of metals on other surfaces provided that the redox potentials are favorable. For example, the selective chemical vapor deposition of Pd from Pd(hfac)₂ on Cu and Fe substrates occurs by similar redox transmetallization reactions. We are continuing to explore this novel, selective CVD route to films of Ag, Pd, and other metals on copper and other metal surfaces.

Experimental

The apparatus used in the CVD of the Ag films is described as CVD1 elsewhere.^{22,23} The Auger electron spectra were recorded on a Physical Electronics PE 595 system with a beam energy of 3 kV and a beam current of ca. 5 μA and scanning electron micrographs were obtained on an ISI DS-130 instrument by Wenbin Lin. Microanalyses were performed by the University of Illinois Microanalytical Laboratory and the mass spectra were recorded by the University of Illinois Mass Spectrometry Laboratory.

References

1. Green, M. L.; Levy, R. A. *J. Metals* 1985, 37, 63-71.
2. Shin, H. K.; Chi, K. M.; Hampden-Smith, M. J.; Kostas, T. T.; Farr, J. D.; Paffett, M. *Angew. Chem., Advanced Mater.* 1991, 3, 246-248.
3. Jain, A.; Chi, K. M.; Kostas, T. T.; Hampden-Smith, M. J.; Farr, J. D.; Paffett, M. *Chem. Mater.* 1991, 3, 995-997.
4. Norman, J. A. T.; Muratore, B. A.; Dwyer, D. N.; Roberts, D. A.; Hochberg, A. K. *J. De Physique IV*, 1991, 1, 271.
5. Reynolds, S. K.; Smart, C. J.; Baran, E. F.; Baum, T. H.; Larson, C. E.; Brock, C. J. *Appl. Phys. Lett.* 1991, 59, 2332.
6. Chi, K. M.; Garvey, J. W.; Shin, H. K.; Hampden-Smith, M. J.; Kostas, T. T.; Farr, J. D.; Paffett, M. F. *J. Mater. Res.* 1991, 7, 261.
7. Dubois, L. H.; Zegaraki, B. R. submitted to *J. Electrochem. Soc.*
8. Powell, C. F.; Oxley, J. H.; Blocher, Jr., J. M. *Vapor Deposition*; John Wiley & Sons: New York, 1986; pp 256-257.
9. Voorhoeve, R. J. H.; Merewether, J. W. *J. Electrochem. Soc: Solid-State Science and Technology* 1972, 119, 364-368.
10. Tsao, K. Y.; Busta, H. H. *J. Electrochem. Soc: Solid-State Science and Technology* 1984, 131, 2702-2708.
11. Bent, B. E.; Nuzzo, R. G.; Dubois, L. H. In *Laser and Particle-Beam Chemical Processing for Microelectronics*; Ehrlich, D. J.; Higashi, G. S.; Oprysko, M. M. Eds.; *Mater. Res. Soc. Symp. Proc.* Materials Research Society: Pittsburgh, 1988; Vol. 101, pp 177-182.

12. Anon. *Res. Discl.* 1986, 263, 146.
13. Anon. *Res. Discl.* 1986, 261, 61.
14. Oehr, C.; Suhr, H. *Appl. Phys. A* 1989, 49, 691-696.
15. Jeffries, P. M.; Girolami, G. S. submitted to *Chem. Mater.*
16. Gupta, D.; Campbell, D. R.; Ho, P. S. In *Thin Films: Interdiffusion and Reactions*; Poate, J. M.; Tu, K. N.; Mayer, J. W. Eds.; John Wiley & Sons: New York, 1986; Chapter 7.
17. Bertrand, J. A.; Kaplan, R. I. *Inorg. Chem.* 1966, 5, 489-491.
18. Shin, H. K.; Chi, K. M.; Hampden-Smith, M. J.; Kodas, T. T.; Farr, J. D.; Paffett, M. F. In *Chemical Perspectives of Microelectronic Materials II*; Interrante, L. V.; Jensen, K. F.; Dubois, L. H.; Gross, M.E., Eds.; *Mat. Res. Soc. Symp. Proc.*; Materials Research Society: Pittsburgh, 1991; Vol. 204, pp 421-426.
19. Morris, M. L.; Moshier, R. W.; Sievers, R.E. *Inorg. Chem* 1963, 2, 411-412.
20. Clobes, A. L.; Morris, M. L.; Koob, R. D. *Org. Mass Spectrom.* 1971, 5, 633.
21. Reichert, C.; Westmore, J. B.; Gesser, H. D. *J. Chem. Soc., Chem Commun.* 1967, 782-783.
22. Gosum, J. E. Ph.D. Thesis, University of Illinois at Urbana, March 1991.
23. Jensen, J. A. Ph.D. Thesis, University of Illinois at Urbana, May 1988.